# On silica's roles in controlling americium migration in contaminated sediments

Calvin H. Delegard [a], Carolyn I. Pearce [b], Hilary P. Emerson [b,*]

[a] TradeWind Services, LLC, Richland, WA, 99352, USA
[b] Pacific Northwest National Laboratory, Richland, WA, 99352, USA

ARTICLE INFO

Editorial handling by: Daniel S Alessi

ABSTRACT

Two studies in the early 1980s described the leaching behavior of americium (Am) disposed as part of acidic, high-salt processing wastes from the Hanford Site's Plutonium Finishing Plant to nearby surface sediments. Batch leach experiments showed that the Am concentrations followed a linear log [Am] versus pH relationship with a slope of −1. However, column leach experiments in a second study did not follow this relationship, and only ~30% of the americium was removed even after extensive column leaching. In this study, the 1980s research is re-examined along with previously unpublished information. Additionally, by considering recent published work, a plausible mechanism is proposed to explain these phenomena. Amorphous silica in the contaminated sediments is postulated to be the substrate responsible for both the exchangeable Am available for leaching and the retained, low-leachable Am made evident in the column leach experiments. The exchangeable $Am^{3+}$ in the contaminated sediment leach experiments behaves with pH dependence similar to that observed for uptake onto amorphous silica of sodium ($Na^{+}$), calcium ($Ca^{2+}$), barium ($Ba^{2+}$), cadmium ($Cd^{2+}$), uranyl ($UO_2^{2+}$), ferric ($Fe^{3+}$), chromic ($Cr^{3+}$), cupric ($Cu^{2+}$), plumbous ($Pb^{2+}$), uranium(IV) ($U^{4+}$), plutonium(IV) ($Pu^{4+}$), zirconium ($Zr^{4+}$), analogue lanthanide (gadolinium, $Gd^{3+}$, europium, $Eu^{3+}$, and lutetium, $Lu^{3+}$) and curium ($Cm^{3+}$) ions, as well as other studies with $Am^{3+}$. Correspondingly, the residual low-leachable $Am^{3+}$ revealed in the column leach experiments is attributed to incorporation of $Am^{3+}$ within amorphous silica by dynamic $Am^{3+}$ sorption and silica precipitation processes which occurred under extreme conditions during waste interaction with sediments.

## 1. Introduction

Rai et al. (1981) and Delegard et al. (1982) described the geochemical behavior of americium (Am) from ground disposal of acidic, high-salt processing wastes from the Hanford Site's Plutonium Finishing Plant (PFP) (see also Figure S1, Emerson et al., 2021). The wastes arose from tributyl phosphate (TBP) solvent extraction recovery of Am-bearing scrap plutonium from nitric acid solutions. The studies examined sediments from the 216-Z-9 (Z-9) enclosed trench, which received wastes from the RECUPLEX Process (Rai et al., 1981) and sediments from the 216-Z-1A (Z-1A) tile field, which received similar wastes from the later processing at the Plutonium Reclamation Facility (PRF; Delegard et al., 1982).

Batch contact leaching experiments of contaminated sediments in the two studies showed strikingly similar behaviors for Am, with the two studies' log [Am]-versus-pH data overlying each other at a slope near −1. However, column leaching of the Z-1A sediment did not show the same log [Am]-pH relationship (Delegard et al., 1982). Furthermore, even after extensive column leaching, about 70% of the Am still was retained on the sediment.

The present study re-examines the Rai et al. (1981) and Delegard et al. (1982) research, brings to light previously unpublished information from the Delegard et al. experiments, and connects current technical literature to answer the following questions regarding Am fate in the Hanford Site PFP waste sites:

1. What causes the observed log [Am] versus pH relationship in batch solution contacts with contaminated sediments?
2. Why, despite the batch behavior, does most of the Am still remain in the sediment even after extensive column leaching?

## 2. Prior characterization of americium fate following acidic plutonium waste disposal

During its lifetime (1955–1962), the Hanford 216-Z-9 waste disposal

* Corresponding author.
*E-mail address:* hilary.emerson@pnnl.gov (H.P. Emerson).

facility, an enclosed trench subsequently referred to as Z-9, received around 4 million liters of high ionic strength, acidic waste solution containing about 90 kg plutonium (Pu) and 2.3 kg Am from the TBP solvent extraction recovery of scrap Pu by the RECUPLEX[1] Process at the PFP (Delegard et al., 2019). The acidic waste solution (~2.5 M nitric acid, $HNO_3$) was adjusted to pH 2.5 using sodium hydroxide (NaOH) solution prior to discharge to Z-9, partially neutralizing the $HNO_3$ and converting the contained ferric ion ($Fe^{3+}$) to $FeOH^{2+}$ (i.e., the $Fe^{3+}$ hydrolysis reaction). The pH-adjusted waste contained cations; including sodium ($Na^+$), aluminum ($Al^{3+}$), magnesium ($Mg^{2+}$), calcium ($Ca^{2+}$), $FeOH^{2+}$; lesser concentrations of other metal cations (chromium, $Cr^{3+}$, nickel $Ni^{2+}$, mercury, $Hg^{2+}$, and cadmium $Cd^{2+}$); and significant acid capacity primarily as $Al^{3+}$. Anions in the disposed waste were dominated by nitrate ($NO_3^-$), and also included chloride ($Cl^-$), fluoride ($F^-$), and lesser sulfate ($SO_4^{2-}$) (Table 4 in Delegard et al., 2019).

In batch leach studies, Rai et al. (1981) contacted 2 g of water-washed sediment samples, Z9-4-5A and Z9-4-11A, taken from the upper 15.2 cm of the Z-9 trench (Ames 1974) with 20 mL of 0.0015 M $CaCl_2$ (i.e., 100 g/L). The washed Z9-4-5A and Z9-4-11A samples contained 2.29 mg $^{241}Am\ kg^{-1}$ and 4.34 mg $^{241}Am\ kg^{-1}$ sediment (or $9.5 \times 10^{-9}$ and $1.8 \times 10^{-8}$ mol $^{241}Am/g$ sediment), respectively. The contact solution pH ranged from 3.5 to 4.3, indicating that residual acid remained in the water-washed, waste-amended sediments, which in their natural state (prior to reaction with wastes) would have pH ~8. These sandy sediments were from the Hanford Formation with the pH controlled naturally by low concentrations of calcite (1.6 wt% calcite within Hanford Formation sediments in the 200 West Area of the Hanford Site; Table A.1 of Xie et al., 2003). The sediment suspensions in 0.0015 M $CaCl_2$ then were adjusted to pH 3 through 8 using HCl or NaOH solution and allowed to equilibrate for up to 707 days. The Am concentrations and pH values for each test were monitored periodically over this interval. As shown in Fig. 1, apparent equilibria were attained within a day, with log [Am] correlating linearly with pH at slope near − 1.

Rai et al. (1981) established that the log [Am] versus pH data for the two different Z-9 sediment samples (Fig. 1) were statistically indistinguishable. Thus, the data were combined to generate Equation (1).

$$\log[\mathrm{Am, M}] = -(3.76 \pm 0.24) - (1.07 \pm 0.04)\,\mathrm{pH} \quad (1)$$

Rai et al. (1981) also interpreted others' findings of Am uptake onto a wide variety of silicate minerals (i.e., illite, hornblende, augite, kaolinite, quartz, albite, olivine, biotite, bytownite, and microcline) and found that the data selected from the literature adhered reasonably well to the log [Am]-pH correlation, Equation (1), exhibited by leaching the Z-9 sediments.[2]

Similar batch leach studies were conducted concurrently using unwashed Am-contaminated sediment samples from the related nearby PFP waste disposal tile field Z-1A (Delegard et al., 1982). Both Delegard et al. (1982) and Rai et al. (1981) noted that the log [Am] versus pH plot for Z-1A batch tests followed Equation (1). The sediment samples used in the Z-1A tests, collected from below the central discharge lines about 9 m deep in the soil column, contained 100 nCi $^{241}Am/g$ sediment ($1.21 \times 10^{-10}$ mol $^{241}Am/g$), ~1% of the concentrations found in the more surficial Z-9 sediment samples Z9-4-5A and Z9-4-11A, and had 107 nCi $^{239}Pu/g$ sediment ($7.68 \times 10^{-9}$ mol $Pu_{total}/g$) for a Pu/Am mass ratio of 63. The waste solution received in the Z-1A tile field contained 57 kg Pu and 1 kg Am (i.e., nearly the same mass ratio as in the Z-1A sediment sample used in the leach tests, thus indicating equivalent Pu and Am migration rates) and arose from the TBP solvent extraction recovery, from May 1964 until April 1969, of both weapons- and reactor-grade Pu at the PRF (Sections 12 and 15 of Gerber 1997). Overall, ~184 kg Pu (Owens 1981) and an estimated 6.7 kg of co-disposed and in-grown Am remain in Hanford sediments at Z-9, Z-1A, and other in-ground structures from PFP processes.

The 5.2 million liters of waste solution disposed to Z-1A was also adjusted to pH 2.5 before discharge and contained $Na^+$, $Al^{3+}$, $Fe^{3+}$, $Mg^{2+}$, and $Ca^{2+}$ with $NO_3^-$ and $F^-$ (Section 3.2 of Delegard et al., 2019). Overall, the PRF wastes discharged to Z-1A had the same constituents and pH but lower ionic strength than the RECUPLEX wastes discharged to Z-9. Both waste streams also contained co-disposed carbon tetrachloride ($CCl_4$), TBP, and DBBP (dibutylbutyl phosphonate, an extractant used for raffinate polishing) at about 10%, 0.5%, and 0.6–0.8%, respectively, of the total nitrate molar quantities. The two disposed waste compositions are compared in Table 1. With time, $CCl_4$ and TBP/DBBP radiolysis and hydrolysis produced chloride ($Cl^-$) and phosphate ($PO_4^{3-}$), respectively, in the discharged wastes.

Although results from Am concentration-versus-pH batch experiments have been published (Delegard et al., 1982), additional unpublished experimental detail and results from supplementary tests from the same 1980s study are presented here. The primary batch leach experiments with the as-received dry sediments were conducted at room temperature under the following conditions:

1. Sediment/solution ratios of ~0.5–1 g/mL (~500–1000 g/L)
2. Leachants of distilled deionized water (DI water); 0.01, 0.1 and 1 M $CaCl_2$ (calcium chloride); 0.01, 0.1, and 0.3 M $Al(NO_3)_3$ (aluminum nitrate); and 0.01, 0.1, and 1 M NaF (sodium fluoride)
3. Contact times varied from two min to eight days.

The tests with varied electrolytes were performed to determine if any of the dominant waste cations ($Al^{3+}$, $Ca^{2+}$, $Na^+$) or anions (nitrate, chloride, fluoride) influenced Am behavior. All of the primary Z-1A soil batch leach tests had Am concentrations above the $1.4 \times 10^{-10}$ M detection limit except the 1 M NaF test at pH 10.43. Aside from the impacts of the leach solutions, no further adjustments to pH, such as addition of $HNO_3$ or NaOH solution, were made.

Passing the Z-1A leachates through Amicon CF-30 polysulfone cone filters (30,000 molecular weight cut-off; about 8 nm) left the Am concentrations unaltered (Delegard et al., 1982). Therefore, the Am carried in the solution was not present as a colloid. The Am solution species were found to be cationic in DI water leaching, as shown by sorption onto cation exchange resin. The sole consistent effect of leachant composition on Am concentration was to alter pH. The sediment/DI water mixture pH was 3.86. Adding $CaCl_2$ or $Al(NO_3)_3$ decreased pH, the effect increasing with concentration and greater for $Al^{3+}$, as would be expected by metal ion hydrolysis. In contrast, NaF increased pH, with pH change greater as NaF concentration increased, reflecting the fact that $F^-$ is the conjugate of hydrofluoric acid (HF), a weak acid. The leach experiments using DI water; 0.01, 0.1, and 1 M $CaCl_2$; 0.03, 0.1, and 0.3 M $Al(NO_3)_3$; or 0.01 and 0.1 M NaF solutions (Fig. 2) equilibrated in Am concentration and pH within minutes to hours. The first three data points for each condition were at 2, 8, and 30 or 35 min. Although drift in pH and Am concentration occurred with time, generally more so for

[1] A definitive explanation of the term RECUPLEX has not been found but likely is related to the original dual missions of RECUPLEX – the recovery and purification of Pu from scrap in the PFP and coupling this purification process to the final Pu purification stages of the Hanford reprocessing plants. In the end, the latter mission was not implemented (Delegard et al., 2019).

[2] The tests with illite used 0.15 M $CaCl_2$ and 0.3 and 5.1 M NaCl leachants, were run at pH 2.3 to 6 with less than 30 days contact time (Relyea et al., 1979) and adhered to the correlation shown in Equation (1) (Fig. 3 of Rai et al., 1981). Tests with 0.03 M $NaHCO_3$ leachant in the same paper clustered around $5 \times 10^{-10}$ M Am and pH 8.5. Although Am concentrations in the $NaHCO_3$ tests were about 1000-times greater than predicted by Equation (1), they were near the Am detection limit and thus had high uncertainty. It is likely that the greater Am concentrations were due to carbonate complexation of the $Am^{3+}$. Similarly, Allard et al. (1980) conducted 5-day contact tests of Am-bearing solutions with the other silicate minerals. These data also followed Equation (1) and used a synthetic groundwater adjusted to pH ~4 to 9 (Fig. 4 of Rai et al., 1981). Positive deviations from the prediction given by Equation (1) were shown above pH 7. These high values likely also were due to carbonate complexation of $Am^{3+}$.

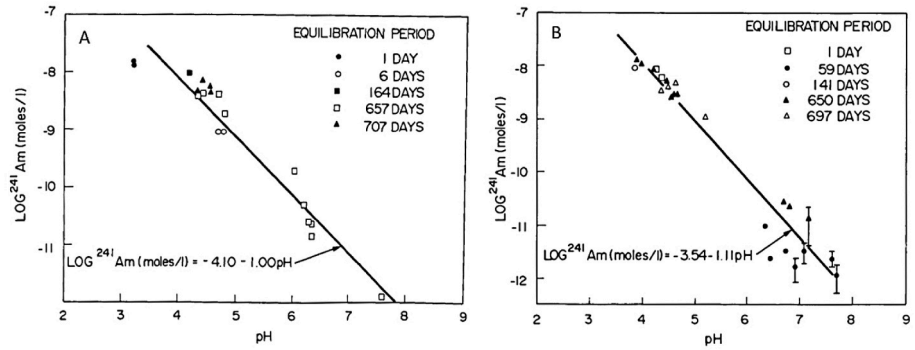


**Fig. 1.** Effect of pH on Am Concentration for Z9-4-5A (A) and Z9-4-11A (B) Sediment Samples Contacted with 0.0015 M $CaCl_2$ Solution (Rai et al., 1981).

the more dilute solutions, the log [Am] values as functions of pH clearly followed the correlation determined by Rai et al. (1981) for Z-9 sediments and other minerals as expressed by Equation (1).

The equilibrium shown in Equation (2) was hypothesized by Rai et al. (1981) to explain Am concentrations in their tests of RECUPLEX waste-altered Hanford sediment minerals, the tests on Am uptake onto illite by Relyea et al. (1979), the Am uptake tests on a variety of silicate minerals by Allard et al. (1980), and early results of tests of PRF waste-altered minerals ultimately published by Delegard et al. (1982):

$$Am_{soil} + H^+ \rightleftharpoons Am(OH)_2^+ \quad (2)$$

While Rai et al. (1981) did not identify the hypothesized solubility-controlling solid phase, $Am_{soil}$, they concluded "that the final Am concentrations in solutions are limited by a reaction that appears to be common to all the rocks, minerals, soils and sediments".

Although the equilibrium given in Equation (2) shows the observed −1 slope dependence of log [Am] versus pH, the $Am(OH)_2^+$ dissolved species hypothesized by Rai et al. (1981) is unlikely over the experimental pH 3 to 8 range. The midpoint of the first hydrolysis of $Am^{3+}$ does not occur until about pH 7.2, as shown in Equation (3), and the second hydrolysis, to form $Am(OH)_2^+$, at pH ~7.7, as shown in Equation (4) (Brown and Ekberg 2016):

$$Am^{3+} + H_2O \rightleftharpoons AmOH^{2+} + H^+ \log K = -7.22 \pm 0.03 \quad (3)$$

$$AmOH^{2+} + H_2O \rightleftharpoons Am(OH)_2^+ + H^+ \log K = -7.7 \pm 0.2 \quad (4)$$

Therefore, if a solubility equilibrium like that described by Equation (2) is occurring, the dissolved Am species must not be $Am(OH)_2^+$ but instead a different singly charged positive complex. As shown later, $AmCO_3^+$ is not plausible until about pH 7.

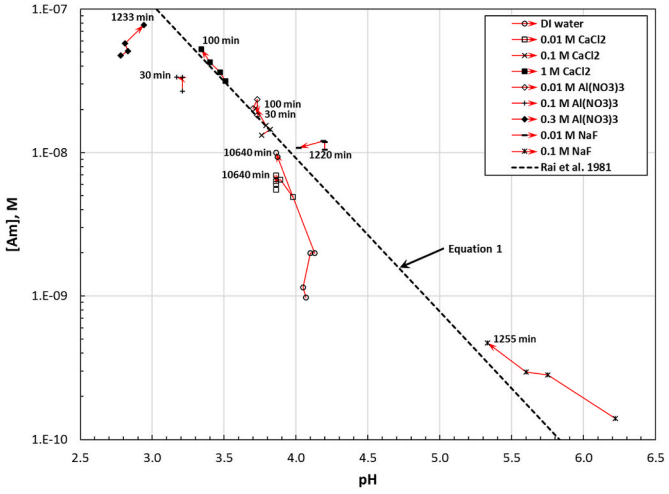


**Fig. 2.** Batch contact leaching of Am from Z-1A soil compared with Equation 1.

Other Am-bearing solid phases – $Am(OH)_3$, Am within $PuO_2 \bullet xH_2O$ (am), and $AmPO_4 \bullet xH_2O$ – may be considered as potential solubility controls. However, as already noted by Rai et al. (1981), the $\sim 10^{-11}$ M Am concentration at pH 7 in the two Z-9 sediments observed by Rai et al. (1981) is much too small to be controlled by the solubility of $Am(OH)_3$, which is $\sim 10^{-4}$ to $10^{-5}$ M at pH 7 (Figures 12–3 and 12-4 of Guillaumont et al., 2003). The solubility of $Am(OH)_3$ also has a 3-fold more steep concentration dependence on pH than observed in the 1980s Am-contaminated sediment testing. Control of Am concentration by its dissolution from within plutonium(IV) hydrated oxide, $PuO_2 \bullet xH_2O$ (am), also might be considered. The solubility of $PuO_2 \bullet xH_2O$(am) as a function of pH in aerated conditions has been studied by numerous parties with the results showing, to a first approximation, that [Pu] decreases from about $10^{-3}$ M to $10^{-7}$ M at pH ~3 to 7; i.e., a slope of about −1 in log [Pu]-versus-pH (Neck et al., 2007). However, most of the Am present in the wastes disposed to Z-9 and Z-1A arrived not within $PuO_2 \bullet xH_2O$(am) particles but as free $Am^{3+}$ from scrap dissolution and Pu recovery processes. Therefore, control of [Am] by its incorporation within $PuO_2 \bullet xH_2O$(am) particles is unlikely.

The synthesis of $AmPO_4 \bullet xH_2O$ and its solubility as a function of pH have been examined (Rai et al., 1992). Recent measurements of Am concentrations, phosphate concentrations, and pH in water equilibration tests of three different Z-9 sediment samples, including the two tested by Rai et al. (1981), show only one sample (Z9-4-5A; the other two were Z9-4-11A and B1HK-42, a sample retrieved about 25 m below the waste discharge surface) could have been saturated in $AmPO_4 \bullet xH_2O$ according to calculated saturation indices (Emerson et al., 2022). In subsequent calculations, saturation indices for tests outlined in Table 1 of Rai et al. (1981) for Z9-4-5A and Z9-4-11A also predict oversaturation in $AmPO_4 \bullet xH_2O$ with saturation indices of 0.91 and 0.5, respectively.[3] The available free phosphate in the 1980s Z-1A tests arising from unknown extents of radiolytic and hydrolytic TBP and DBBP degradation, tempered by phosphate precipitation with $Mg^{2+}$, $Ca^{2+}$, $Al^{3+}$, and $Fe^{3+}$ from the wastes (Table 1) and calcium from the sediments, is impossible to predict. The phosphate concentration itself was not measured in these 1980s tests. As will be demonstrated, however, strong evidence exists

[3] Saturation index calculations were performed using the thermodynamic database file thermo.com.V8.R6+.dat that is supplied with Geochemist's Workbench version 10 but augmented with the selected data from the Organization for Economic Co-operation and Development/Nuclear Energy Agency-Thermochemical Database Project (NEA TDB) (Lemire et al., 2001; Guillaumont et al., 2003; Grenthe et al., 2020). The saturation index is defined as log (Q/Ksp), where Q is the activity product and Ksp is the mineral solubility product at equilibrium at the temperature of interest. Values of zero are at equilibrium where more positive values are considered oversaturated and negative values are considered undersaturated with respect to the pertinent solid phase.

that Am concentration is controlled by other processes besides compound solubility.

Delegard et al. (1982) also described two parallel saturated column leaching tests of the same contaminated Z-1A sediment as used in the batch tests. The column tests were performed to determine the extent of Am mobilization under groundwater intrusion or massive surface infiltration conditions. The surface flood was simulated using 0.01 M $CaCl_2$ solution (30 mM ionic strength; pH 6.2) and the Hanford-affected (i.e., nitrate-bearing) groundwater was simulated using ~1.0 mM $Na^+$, 0.17 mM $K^+$, 0.5 mM $Mg^{2+}$, 0.5 mM $Ca^{2+}$, 1.1 mM $H_4SiO_4$, 0.7 mM $NO_3^-$, 0.4 mM $SO_4^{2-}$, and 1.3 mM $HCO_3^-$ (4.5 mM ionic strength; pH 8.1), a composition based on the average concentrations observed in 62 nearby wells from circa 1980. To ensure saturation of the sediment solids with leachant, the leach solutions were pumped vertically upwards into the bottoms of identical 2.5-cm-diameter and 22-cm-long glass columns at ~2.6 cm/h linear flow rate. Each 102.4 $cm^3$ sediment column volume contained 180 g of 2.64 $g/cm^3$ particle density sediment leaving 34.2 $cm^3$ pore volume. Each column test ran 60 days at about 5.1 $cm^3$ leachant/hour, to give a residence time in the column of (34.2/5.1 = ) 6.7 h. The effluent solutions were analyzed for pH, Am, and Pu concentrations.

The Am concentrations in unfiltered solutions versus pH observed in the Delegard et al. (1982) column leach tests are shown in Fig. 3. Spot checks showed filtered (Amicon CF-30 polysulfone cone filters) and unfiltered solutions had experimentally indistinguishable concentrations, thus showing negligible Am transport by colloids. Also plotted are the batch test concentrations according to Equation (1) based on Z-9 observations (Rai et al., 1981). Fig. 3 illustrates that the Am concentrations initially were about 10-times above the concentrations expected based on batch tests. More than 80% of the Am ultimately leached was removed in the first of the 210 leachant pore volumes passed through each column. The prominent Am surge also showed marked cation elution and pH as low as 3.5, lower even than in simple batch tests with water (pH ~3.9) or the more dilute batch leachants. The pH generally increased with further added leachant, but the waste-affected sediment, even after 210 column volumes, remained buffered well below the pH ~8 normally found in native Hanford Site sediments. The simulated groundwater solution, which contained 1.3 mM $HCO_3^-$, partially neutralized the contaminated sediment acidity to attain higher pH than the 0.01 M $CaCl_2$ leachant. The Am concentrations for both the simulated groundwater and 0.01 M $CaCl_2$ leachants initially decreased and pH increased. The 0.01 M $CaCl_2$ leachates plateaued at lower pH, ~4.2 to 4.8, and higher Am concentration, (1–2) $\times 10^{-10}$ M, than did the simulated groundwater, which ended at pH ~5.3 and ~$3 \times 10^{-12}$ M Am. However, even after 210 pore volumes, ~70% of the Am and 99% of the Pu remained associated with the sediment in each column and thus unavailable, or only poorly available, for leaching.

Delegard et al. (1982) hypothesized that the high Am concentrations in the initial column effluents, compared with the concentrations expected based on batch leaching, were due to a complexing agent that was present in the disposed waste and concentrated at the solution front, resulting in enhanced Am leaching. However, candidate suspected complexing agents were not identified.

## 3. Characterization of waste-altered sediments and the prevalence of amorphous silica

A constituent ubiquitous to all silicate rocks, minerals, soils, and sediments is amorphous silica, expressed as silica gel, $H_4SiO_{4\ (am)}$ or $Si(OH)_{4\ (am)}$. Amorphous silica, which develops by weathering of more complex silicate minerals (Kasting 2019), is present at about 0.1 wt% from inorganic sources and about 1 wt% from biotic sources in glacial till and quaternary sediments found elsewhere (Alfredsson et al., 2016; see also the SI) that are broadly similar to the Hanford Formation sediments. No information was found, however, on concentrations of amorphous silica in the near-surface Hanford Formation sediment beds wherein the Z-9 and Z-1A disposal sites are located.

Besides the amorphous silica present naturally in Hanford sediments, amorphous silica arises by acid hydrolysis of sediment minerals, especially the abundant glassy basalt groundmass, by the low pH, high salt, solvent extraction wastes such those disposed to the RECUPLEX Z-9 trench and PRF Z-1A tile field sediments. Alteration of glassy areas in basalt fragments by depletions in Al, Ca, Fe, potassium (K), and Mg leaving relatively unchanged silicon (Si), and titanium (Ti) concentrations near the waste-altered surfaces of Z-1A sediments are shown in Fig. 4 (taken from Fig. 6 of Price and Ames, 1976).[4]

Significantly, the regions of highest radioactivity shown in the autoradiograph at the top middle of Fig. 4 correlate with the Al-, Ca-, Fe-, K-, and Mg-depleted but silica-rich chemical alteration zones. Price and Ames (1976) argued that the focused radiographic darkening at the residual silica-rich surface arose from Pu precipitation caused by local pH increase from the basalt-waste reactions. However, the darkening likewise could have come from Pu exchange onto the abundant silanol groups present in the residual silica gels from acid attack of the glassy basalt groundmass. Price and Ames (1976) also allowed that the autoradiolytic record is not limited to Pu and may have been augmented by Am radiolytic contributions (which would have been 10–20% of the Pu specific alpha activity; Figures 24 and 25 of Delegard et al., 2019, derived from Table I and Appendix An of Price et al., 1979). Therefore, acid-attacked silica-rich altered mineral regions correspond to high Pu (and perhaps Am) deposition.

In addition to the silica gel from altered minerals, silica gels arise from $HNO_3$ dissolution of the silicate-bearing scrap fed to RECUPLEX and PRF, both as a separable solid phase (after coagulation) and as a significant contributor to solvent extraction interfacial crud (Section 2.3.7 of Delegard et al., 2019). Thus, the contaminated sediments contain at least three amorphous silica sources – that native to the sediments, from acid hydrolysis of the sediments, and from in-plant processing of silicate-bearing scrap. Based on its ubiquity, high expected concentrations in the waste-affected sediments, and associated high surface area, we suggest that amorphous silica could be the unidentified solid phase hypothesized by Rai et al. (1981) controlling Am solution concentration.

Beyond its presence in the solid phase, amorphous silica buffers dissolved silica concentration to ~2 (±0.4) $\times 10^{-3}$ M in water at pH 1 to 9 (Alexander et al., 1954), encompassing the pH range observed for Z-9 and Z-1A waste site sediments. Dissolved silica concentrations decrease somewhat in strong acid; silica solubilities in both 2 M $HNO_3$ and 2 M HCl are ~$9 \times 10^{-4}$ M (Felmy et al., 1994). Dissolved silica concentrations increase above pH 9 by formation of the silicate anion, $SiO(OH)_3^-$ (Alexander et al., 1954).

## 4. Am Concentration-controlling reactions based on amorphous silica as described in the technical literature

Because of amorphous silica's prevalence in the sediments of the PFP waste disposal sites, literature on the uptake of various metal ions onto amorphous silica or silica gel was surveyed to compare with the observations collected and cited by Rai et al. (1981) and Delegard et al. (1982) for $Am^{3+}$. In the earliest such work found, Ahrland et al. (1960) studied uptake onto three different silica gels of several cations: $Pu^{4+}$, $Ca^{2+}$, $Na^+$, barium ($Ba^{2+}$), uranyl ($UO_2^{2+}$), uranium ($U^{4+}$), zirconium ($Zr^{4+}$), and the rare earth gadolinium ($Gd^{3+}$). The uptake rates, pH dependencies, and exchange capacities for the three gels also were determined. Uptake rates were lower for highly hydrolyzed metal ions such as $U^{4+}$, $Pu^{4+}$, and $Zr^{4+}$ compared with the less hydrolyzed ions including

[4] As noted by Ames (1974), "hydrolysis of the silicates constituting the Z-9 trench soil was accelerated due to a high concentration of hydrogen ions. Silica is prevalent because its solubility remained low in relation to alumina in the low pH Z-9 environment."

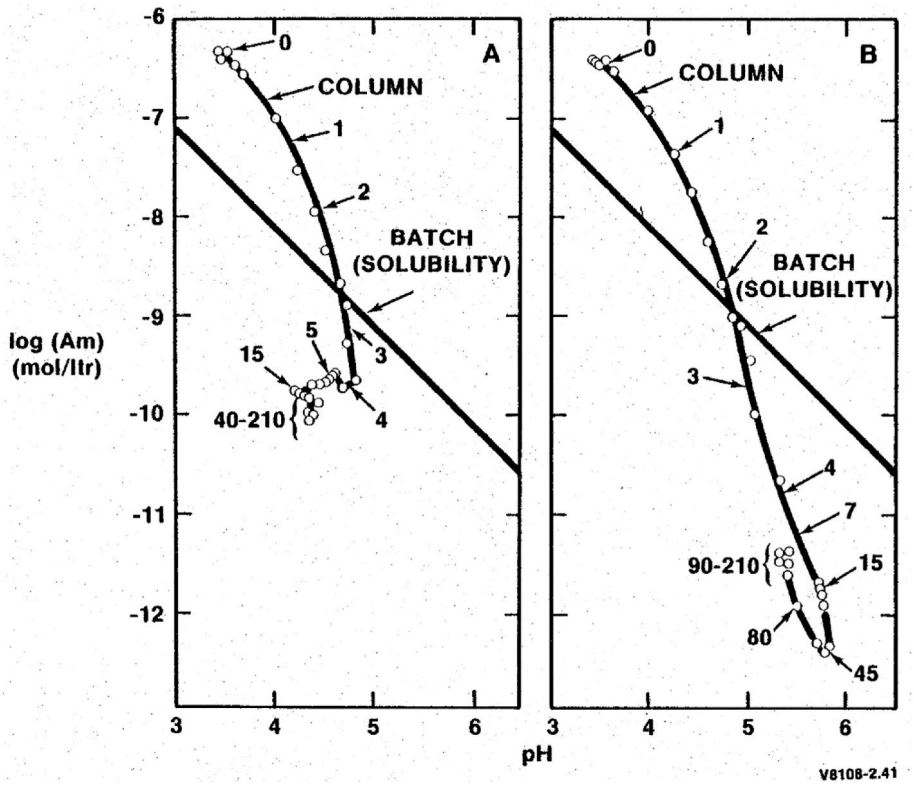


**Fig. 3.** Saturated Column Americium Leaching from 216-Z-1A Sediments Using. A: 0.01 M $CaCl_2$ and B: Simulated Groundwater.
Numbers show throughput column pore volumes (Fig. 1 of Delegard et al., 1982).

$Gd^{3+}$, with equilibrium attained within 1 h for $Pu^{4+}$ but in less than 5 min for $Gd^{3+}$. The three tested silica gels had similar exchange capacities. Although Ahrland et al. (1960) did not study $Am^{3+}$ uptake, $Gd^{3+}$, with identical charge and similar ionic radius as $Am^{3+}$ (0.938 and 0.975 Ångstroms, respectively; Shannon 1976), would be a close analogue.

The metal ions' distribution coefficients, $K_d$s, onto 50–100 mesh silica gel (at 100 g silica gel per liter) were measured from pH ~0 to ~8.3, depending on the ion involved, as shown in their Fig. 6 (Ahrland et al., 1960). These data are replotted here in Fig. 5 for $Zr^{4+}$, $U^{4+}$, $Pu^{4+}$, $UO_2^{2+}$, $Gd^{3+}$, $Ca^{2+}$, and $Na^+$.[5] Equilibration times were not reported, but likely were less than a few days based on the rapid uptake equilibria. They found that log $K_d$ plotted versus pH became linear with near unit (0.85–1.52) slope as sorption approached completion at higher pH and thus the metal concentrations on the solid, $[Me]_{solid}$, became practically invariant.

Under increasing pH conditions, metal ion sorption increases and solution concentrations, $[Me]_{solution}$, decrease. Because metal ion concentration on the solid, $[Me]_{solid}$, tends to a constant value at high loading and high pH, $K_d$ becomes proportional to $1/[Me]_{solution}$ or $[Me]^{-1}_{solution}$. Thus, plots of log $[Me]_{solution}$ versus pH for the Ahrland et al. (1960) data should approach slopes near −1 with increasing pH. Therefore, the $K_d$ values, solid/solution ratios, and starting metal ion concentrations from Ahrland et al. (1960) were used to determine the ions' experimental solution concentrations, in equilibrium with silica gel, with respect to pH. The log $[Me]_{solution}$ with respect to pH as derived from the data of Ahrland et al. (1960) are compared in Fig. 6 with the log [Am]-pH relation observed by Rai et al. (1981) according to Equation (1).

As shown in Fig. 6, log $[Me]_{solution}$ decreases with increasing pH with most slopes near or approaching −1, like that observed by Rai et al. (1981) for $Am^{3+}$, and in accord with the expectations based on the log $K_d$ versus pH analysis described above. The −1 slope was observed irrespective of the metal ion charge: +1 ($Na^+$), +2 ($Ca^{2+}$, $UO_2^{2+}$), +3 ($Gd^{3+}$, $Am^{3+}$), or +4 ($U^{4+}$, $Pu^{4+}$, $Zr^{4+}$). The $Na^+$ slope was not as steep (−0.46), perhaps because the tests did not continue higher to pH ~9 and onset of silica hydrolysis.

The metal ion concentration data plateaus observed by Ahrland et al. (1960) for most metal ions as the pH decreased tend to the respective starting test concentrations (data were inadequate for $Zr^{4+}$), indicating exhaustive metal ion removal from silica gel at higher $H^+$ activities (Fig. 6). For example, the initial Pu(IV) concentration before contact with the silica gel was $1 \times 10^{-5}$ M. The Pu concentration at the lowest measured pH (0) was 91% of the maximum possible concentration or about $9.1 \times 10^{-6}$ M. As noted by Ahrland et al. (1960), the pH values where the respective metal ion concentrations plateau, thus indicating their affinities for silica, correspond with their tendencies to hydrolyze. $UO_2^{2+}$ behaves more like a trivalent metal ion than a divalent ion ($Ca^{2+}$ or the similar $Ba^{2+}$). By this measure, the behaviors of $Gd^{3+}$ (Ahrland et al., 1960) and $Am^{3+}$ (Rai et al., 1981) would be expected to be similar. However, the nature of the solids, the metal ion loadings, and test types (sorption/leaching) differ in these two investigations.

The log $[Ca^{2+}]$ versus pH plot is compared with the dissolution of wollastonite ($CaSiO_3$) according to Equation (5), based on thermodynamic equilibrium values (taken from Table 7.1 of Lindsay 1979). Although the wollastonite log $[Ca^{2+}]$ versus pH plot lies near that of the data derived from Ahrland et al. (1960), it has a slope of −2, reflecting the equilibrium in Equation (5), and not slope of about −1 as observed by Ahrland et al. (1960). Therefore, the $Ca^{2+}$ concentration in the Ahrland et al. (1960) work is not controlled by simple dissolution of $CaSiO_3$.

[5] $Ba^{2+}$ was not evaluated but behaves practically identically with $Ca^{2+}$. The $K_d$ is the concentration of a metal ion, Me, on the solid, $[Me]_{solid}$, divided by the metal ion concentration in solution, $[Me]_{solution}$.

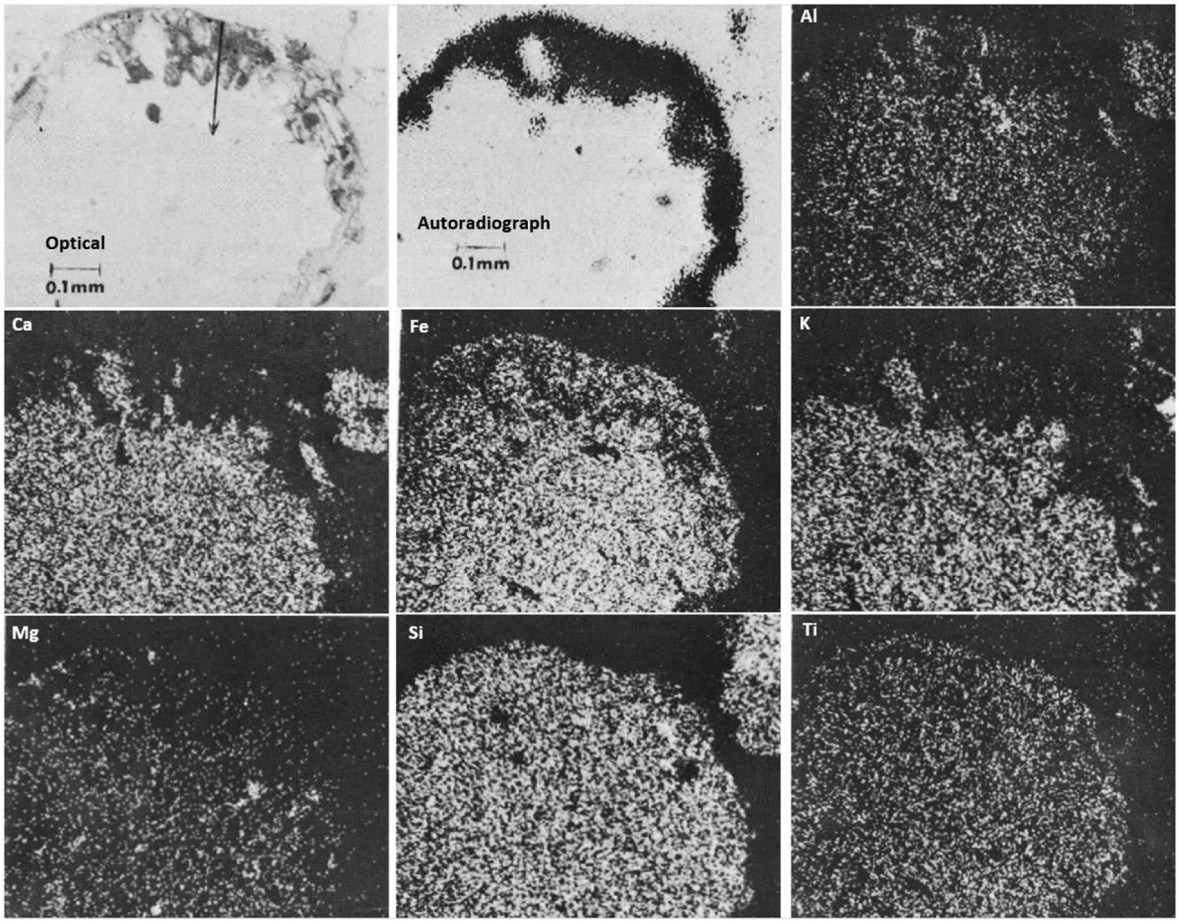


**Fig. 4.** Optical, autoradiograph, and element mapping images of waste-etched Z-1A basalt Particle (from Fig. 6 of Price and Ames 1976).

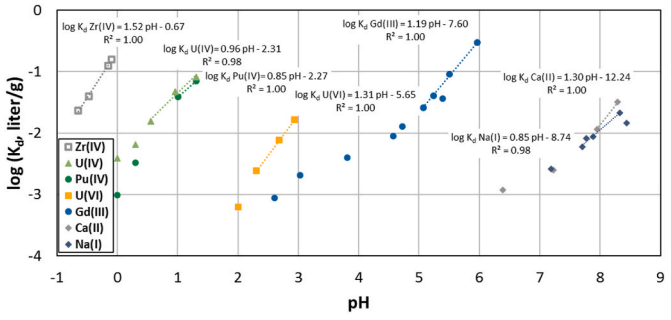


**Fig. 5.** $Na^{+}$, $Ca^{2+}$, $Gd^{3+}$, $UO_2^{2+}$, $Pu^{4+}$, $U^{4+}$, and $Zr^{4+}$ Distribution Coefficients ($K_d = [Me]_{solid}/[Me]_{solution}$) onto Silica as Functions of pH (Ahrland et al., 1960).

$$CaSiO_{3\ solid} + 2\ H^{+} + H_2O \rightleftharpoons H_4SiO_4 + Ca^{2+} \quad (5)$$

Schindler et al. (1976; for $Fe^{3+}$, $Pb^{2+}$, $Cu^{2+}$, and $Cd^{2+}$) and Takahashi et al. (1999; for $Rb^{+}$, $Be^{2+}$, $Sr^{2+}$, $Ba^{2+}$, $Mn^{2+}$, $Co^{2+}$, $Zn^{2+}$, $Sc^{3+}$, $Y^{3+}$, $Ce^{3+}$, $Gd^{3+}$, $Lu^{3+}$, $Cr^{3+}$, and $Fe^{3+}$) conducted tests similar to those of Ahrland et al. (1960) with analogous outcomes (see Supplemental Information Figures S2 and S.3).

Additional literature on the uptake and release of trivalent lanthanides and actinides, especially $Am^{3+}$, onto amorphous silica, silica gel, and quartz was surveyed. Numerous studies were found, many of which are summarized here. Lanthanide data include the $Gd^{3+}$ findings of Ahrland et al. (1960) for uptake onto Kebo silica gel, $Eu^{3+}$ uptake onto Aerosil fumed silica (Takahashi et al., 2006; Kar et al., 2011), and $Eu^{3+}$ uptake onto hydrous silica gel (Pathak and Choppin 2006). For $Am^{3+}$

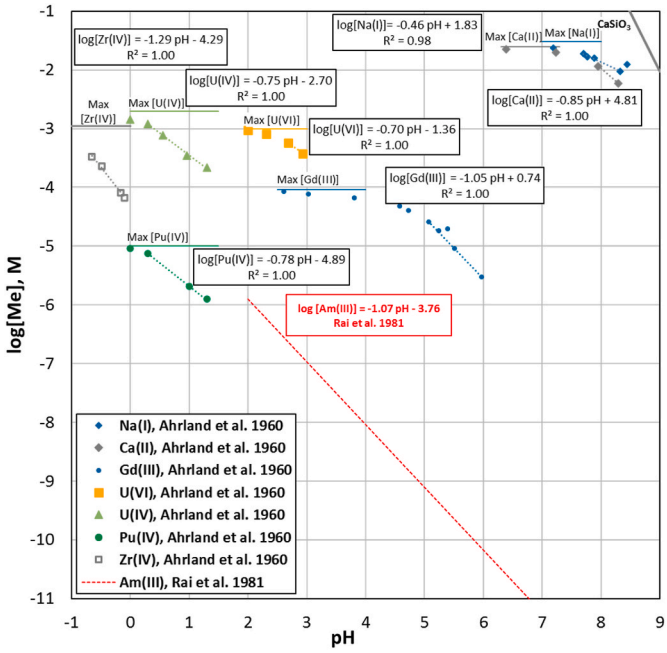


**Fig. 6.** Aqueous Metal Ion Concentrations in Equilibrium with Silica Gel as Functions of pH (Ahrland et al., 1960) Compared with Am Concentrations in Equilibrium with Z-9 Sediments (Rai et al., 1981).

**Table 1**
Compositions of aqueous wastes disposed from RECUPLEX to Z-9 and from PRF to Z-1A.

| Waste Source | Waste Site | Waste Component Concentration, M | | | | | | | |
|---|---|---|---|---|---|---|---|---|---|
| | | $Na^+$ | $Mg^{2+}$ | $Ca^{2+}$ | $Al^{3+}$ | $Fe^{3+}$ | $NO_3^-$ | $F^-$ | $Cl^-$ |
| RECUPLEX | Z-9 | 2.25 | 0.33 | 0.17 | 0.84 | 0.10 | 5.51 | 0.36 | 0.64 |
| PRF | Z-1A | 1.1 | 0.3 | 0.2 | 0.5 | 0.3 | 3.6 | 0.3 | |

From Table 4 and Section 3.2 of Delegard et al., (2019).

uptake tests, the solids included Aerosil 200 amorphous silica (Degueldre and Wernli 1993), Merck amorphous silica (Moulin and Ouzounian, 1992), Sigma-Aldrich amorphous silica (Pathak and Choppin 2007), and, with $Cm^{3+}$, crushed quartz (Stumpf et al., 2008). Most uptake tests had $NaClO_4$ as background electrolyte. The two $Am^{3+}$ leach studies were those of Z-9 sediments by Rai et al. (1981) and of Z-1A sediments by Delegard et al. (1980–1981 unpublished data). Experimental details for the examined trivalent lanthanide and actinide tests are shown in Table 2. Results show that the surface sorption site concentrations in the uptake tests onto silica gel exceed the maximum lanthanide or actinide loading by 100-fold or greater. Therefore, silanol sorption site saturation by the lanthanides and by $Am^{3+}$ and $Cm^{3+}$ did not occur. However, the surface sorption site concentration was near or below the maximum loadings in the $2 \times 10^{-6}$ and $2 \times 10^{-5}$ M $Am^{3+}$ uptake tests onto <5 μm fraction crushed quartz, with evidence found of amorphous or crystalline $Am(OH)_3$ surface precipitation in the test using $2 \times 10^{-5}$ M $Am^{3+}$ (Stumpf et al., 2008).

Silica surface site concentrations are not known for contaminated sediments leached in tests by Rai et al. (1992) and Delegard et al. (1980-81 unpublished data). However, quartz, at ~37%, is abundant in Hanford sediments, with the silicate minerals plagioclase, $NaAlSi_3O_8$ to $CaAl_2Si_2O_8$, at ~20%, and microcline, $KAlSi_3O_8$, at ~16%, comprising the next greatest abundance according to electron microprobe (Table B1 of Xie et al., 2003). The mineral mass based on silicon determined by X-ray fluorescence is ~75% $SiO_2$ (Table A3 of Xie et al., 2003). By reasonably assuming that amorphous silica is at least 0.1 wt% of the native sediment (see SI) and that amorphous silica contains $10^{-3}$ equivalents of sorption sites per gram, the surface site concentrations would be $\geq 10^{-6}$ equivalents per gram of sediment, above site saturation for the available $(9.5–18) \times 10^{-8}$ mol Am/g in the Z-9 tests and $1.21 \times 10^{-10}$ mol Am/g in the Z-1A tests (Table 2). This assumption becomes increasingly conservative based on previous microscopy which identified significant amorphous silica rinds in waste-impacted basalt particles from the Z-1A tile field (Fig. 4 as taken from Figure 6 in Price and Ames 1976).

The log [Me] versus pH plots for the $Am^{3+}$ data of Rai et al. (1981) and Delegard et al. (1980-81 unpublished data) for PFP waste-contaminated sediments are compared with trivalent lanthanide data in Fig. 7. All ions have log $[Me]_{solution}$ versus pH slopes near −1, consistent with the behaviors observed by Ahrland et al. (1960) and Schindler et al. (1976; see SI) for diverse 1+ to 4+ metal ions. Three $Eu^{3+}$ concentration data points at pH ≥6.8 in the study by Takahashi et al. (2006) are lower than expected as extrapolated from the data at pH 5.8–6.7. Because these experiments were conducted in air, the solubility of $EuOHCO_3$, as shown in Fig. 1 in Takahashi et al. (2006), likely was exceeded for these three tests. Analogous $Eu^{3+}$ uptake-on-silica experiments were conducted by Kar et al. (2011) but these did not show apparent solubility limitations even up to pH ~8. Although not explicitly stated, the tests by Kar et al. (2011) seemingly were conducted with carbonate and $CO_2$ excluded.

The log [Me] (metal ion) versus pH plots for the Am leaching data of Rai et al. (1981) and Delegard et al. (1980–1981 unpublished data) for PFP waste-contaminated sediments are compared with published $Am^{3+}$ and $Cm^{3+}$ uptake data on silica gels and <5 μm fraction crushed quartz in Fig. 8. Again, all plots have log $[Me]_{solution}$ versus pH slopes near −1.

In Pathak and Choppin's experiments with $Am^{3+}$, the log [Am] versus pH data overlie each other, even though the background electrolyte concentration was varied at 0.2, 0.5, 1.0, and 1.5 M $NaClO_4$, (Fig. 8, above; Figure 1 of Pathak and Choppin 2007). Analogous observations, not depicted here, were made based on the sparse Am uptake data of Moulin and Ouzounian (1992) at 0.01 and 0.1 M $NaClO_4$. The background electrolyte concentration also did not have an effect on the concentration of $Eu^{3+}$ in 0.02 and 0.1 M $NaClO_4$ (Takahashi et al., 2006). Similarly, data for the Z-1A tests using DI water; 0.01, 0.1, and 1 M $CaCl_2$; 0.01, 0.1, and 0.3 M $Al(NO_3)_3$; and 0.01 and 0.1 M NaF; closely followed Equation (1) irrespective of background electrolyte concentration. The lack of effect of ionic strength and competing cation and anion concentration on $Am^{3+}$ leaching from Z-1A sediments (Delegard et al. 1980-81 unpublished data) and lack of effect of $NaClO_4$ concentration on $Eu^{3+}$ uptake onto silica gel, $Am^{3+}$ uptake onto silica gel, and uptake onto amorphous silica (Takahashi et al., 2006; Pathak and Choppin 2007, and Moulin and Ouzounian, 1992, respectively) implies that, if $Am^{3+}$ interacts with silica by ion exchange, $Na^+$, $Ca^{2+}$, and $Al^{3+}$ have lower affinities for silica than $Am^{3+}$.

Above about pH 7.2, the Pathak and Choppin (2007) Am concentrations deviated positively from the Rai et al. (1981) trend and plateaued at about $5 \times 10^{-11}$ M (see Fig. 8), as observed by Relyea et al. (1979) for $Am^{3+}$ uptake on illite. Pathak and Choppin (2007) postulated that because their tests were performed under $CO_2$-bearing atmospheric conditions, carbonate complexes such as $AmCO_3^+$ could form above pH 7 and thus suppress Am uptake. They bolstered their conclusions by tests showing that the ligands carbonate, oxalate, citrate, and EDTA, in that order, increasingly suppress $Am^{3+}$ uptake by silica.

Degueldre and Wernli (1993) studied $Am^{3+}$ uptake onto amorphous silica colloids (~10 nm primary particle diameter) at 1 g/L concentration in the presence of 0.1 M $NaClO_4$. The impact of carbonate was eliminated by conducting the tests in $CO_2$-free atmospheres. As depicted in Fig. 8, the log [Am] in Degueldre and Wernli's (1993) tests also fell with pH at a −1 slope but the Am concentration at a given pH was about a factor of six greater than observed by Pathak and Choppin (2007) and about 40-fold greater than observed by Rai et al. (1981). A comparison of the log [Am] versus pH plots for these three studies suggests that a lower concentration of silica solids increases the aqueous Am concentration.

Stumpf et al. (2008) studied $Am^{3+}$ and $Cm^{3+}$ uptake onto <5 μm crushed quartz. The experiments were conducted in a $CO_2$-free atmosphere and with carbonate-free solutions at 1 g solid per liter of solution. The initial $Am^{3+}$ concentrations were $2.0 \times 10^{-7}$, $2.0 \times 10^{-6}$, and $2.0 \times 10^{-5}$ M, and the initial $Cm^{3+}$ concentration was $2.0 \times 10^{-7}$ M. The experiments' uptake data with $2.0 \times 10^{-7}$ M initial $Am^{3+}$ and $Cm^{3+}$ showed no discernible differences. This similarity is unsurprising given the ions' identical charges, nearly identical respective ionic radii, 0.975 and 0.97 Å (Shannon 1976), and thus nearly identical chemical properties. Increasing initial $Am^{3+}$ concentrations also led to increased loading onto the quartz solids. The increased loading is manifest in the log [Am]-versus-pH uptake plots (Fig. 8) which begin breaking to lower $Am^{3+}$ concentrations in approximately 1 pH unit increments at pH 5.2, 6.3, and 7.1 for decade increases in initial $Am^{3+}$ concentrations at $2.0 \times 10^{-7}$, $2.0 \times 10^{-6}$, and $2.0 \times 10^{-5}$ M, respectively. As noted, the surface sorption site concentrations were near or below the maximum loadings in the $2 \times 10^{-7}$ and $2 \times 10^{-6}$ M $Am^{3+}$ uptake tests. Evidence for amorphous or crystalline $Am(OH)_3$ surface precipitation was presented for the $2 \times 10^{-5}$ M test (Stumpf et al., 2008).

As shown in Table 2, the batch leaching studies of the contaminated

**Table 2**
Test conditions for trivalent lanthanide and actinide uptake on and leaching from Silica(tes).

| Study Reference | Ion | $[Me]_{max}$, M | Background Electrolyte | Leaching/Uptake Test Type and Solid | [Surface Sites] equiv./g[a] | Solid/Liq. Ratio, g/L | $[Me]_{max}$, moles/g |
|---|---|---|---|---|---|---|---|
| Rai et al., (1981) | $Am^{3+}$ | – | Varied, see text | Leaching Z-9 surface samples Z9-4-5A and Z9-4-11A | Estimated $1 \times 10^{-6}$ | 100 | $9.5 \times 10^{-9}$ $1.8 \times 10^{-8}$ |
| Delegard et al. 1980–1981 | $Am^{3+}$ | – | Varied, see text | Leaching Z-1A 9-m depth samples | Estimated $1 \times 10^{-6}$ | ~500–1000 | $1.21 \times 10^{-10}$ |
| Ahrland et al., (1960) | $Gd^{3+}$ | $9.2 \times 10^{-5}$ | none | Uptake on Kebo chrom. silica gel, 50–100 mesh | $(1.2–1.4) \times 10^{-3}$ | 10 | $9.2 \times 10^{-6}$ |
| Takahashi et al., (2006) | $Eu^{3+}$ | $2.0 \times 10^{-4}$ | 0.02, 0.1 M $NaClO_4$ | Uptake on Aerosil 200 silica gel, 200 $m^2/g$ | $1.45 \times 10^{-3}$ | 8 | $2.5 \times 10^{-5}$ |
| Kar et al., (2011) | $Eu^{3+}$ | $5.0 \times 10^{-5}$ | 0.10 M $NaClO_4$ | Uptake on $SiO_2$ (amorph.), Aerosil silica gel, 180 $m^2/g$ | $2.45 \times 10^{-4}$ | 10 | $5.0 \times 10^{-6}$ |
| Pathak and Choppin (2006) | $Eu^{3+}$ | $2.0 \times 10^{-5}$ | 0.20 M $NaClO_4$ | Uptake on Sigma-Aldrich hydrous silica gel, 675 $m^2/g$ | $\sim 2 \times 10^{-3}$ | 50 | $4.0 \times 10^{-7}$ |
| Degueldre and Wernli (1993) | $Am^{3+}$ | $9.65 \times 10^{-10}$ | 0.10 M $NaClO_4$ | Uptake on $SiO_2$ (amorph.), Aerosil 200 silica gel | $1.45 \times 10^{-3}$ | 1 | $9.65 \times 10^{-10}$ |
| Moulin and Ouzounian, 1992 | $Am^{3+}$ | $1.0 \times 10^{-8}$ | 0.01, 0.1 M $NaClO_4$ | Uptake on Merck amorph. silica gel, 0.075 $m^2/g$ | $2 \times 10^{-6}$ | 10 | $2.5 \times 10^{-9}$ |
| Pathak and Choppin (2007) | $Am^{3+}$ | $4.1 \times 10^{-9}$ | 0.2–1.5 M $NaClO_4$ | Uptake on Sigma-Aldrich amorph. silica gel, 234 $m^2/g$ | $\sim 2 \times 10^{-3}$ | 5 | $8.2 \times 10^{-10}$ |
| Stumpf et al., (2008) | $Cm^{3+}$ | $2.0 \times 10^{-7}$ | 0.10 M $NaClO_4$ | Uptake on crushed quartz, <5 μm fraction, >1 $m^2/g$, 4.6 sites/$nm^2$ quartz surface | $\gtrsim 8 \times 10^{-6}$ | 1 | $2.0 \times 10^{-7}$ |
| Stumpf et al., (2008) | $Am^{3+}$ | $2.0 \times 10^{-7}$ | | | | | $2.0 \times 10^{-7}$ |
| Stumpf et al., (2008) | $Am^{3+}$ | $2.0 \times 10^{-6}$ | | | | | $2.0 \times 10^{-6}$ |
| Stumpf et al., (2008) | $Am^{3+}$ | $2.0 \times 10^{-5}$ | | | | | $2.0 \times 10^{-5}$ |

[a] Aerosil 200 value of $1.45 \times 10^{-3}$ mol of active –OH groups per g from Schindler et al. (1976). The functional group concentrations for the Sigma-Aldrich silica gels in the Pathak and Choppin (2006, 2007) tests of $Eu^{3+}$ and $Am^{3+}$ were not stated but likely are $\sim 2 \times 10^{-3}$ equivalents/g based on comparison with other silica gels of similar surface areas. Functional group concentration for Stumpf et al. (2008) crushed quartz is based on >1 $m^2/g$ surface area and 4.6 sites/$nm^2$.

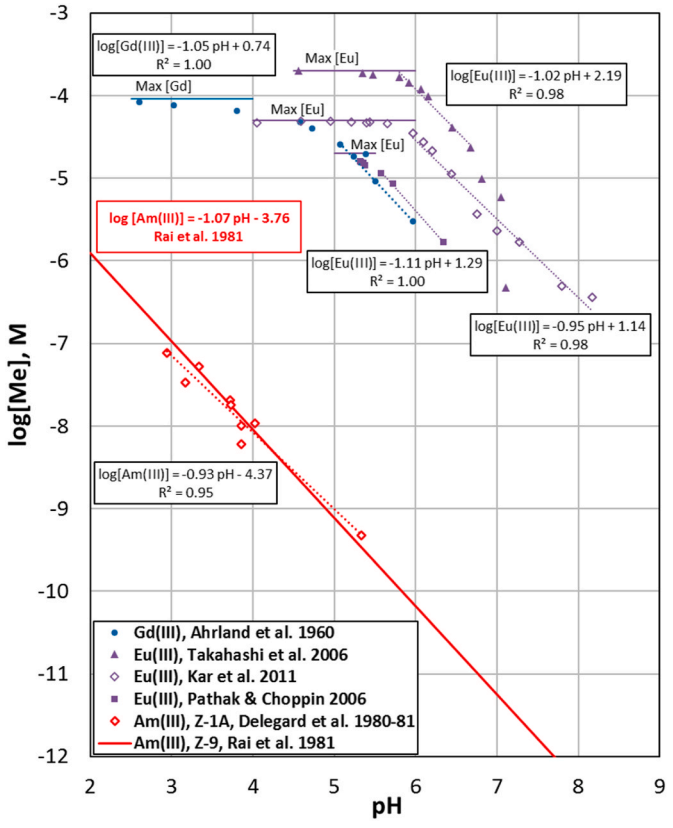


**Fig. 7.** Trivalent Lanthanide Ion Concentrations in Uptake Equilibria with Silica Gel as Functions of pH Compared with Am Concentrations in Leaching Equilibria with Z-9 and Z-1A Sediments.

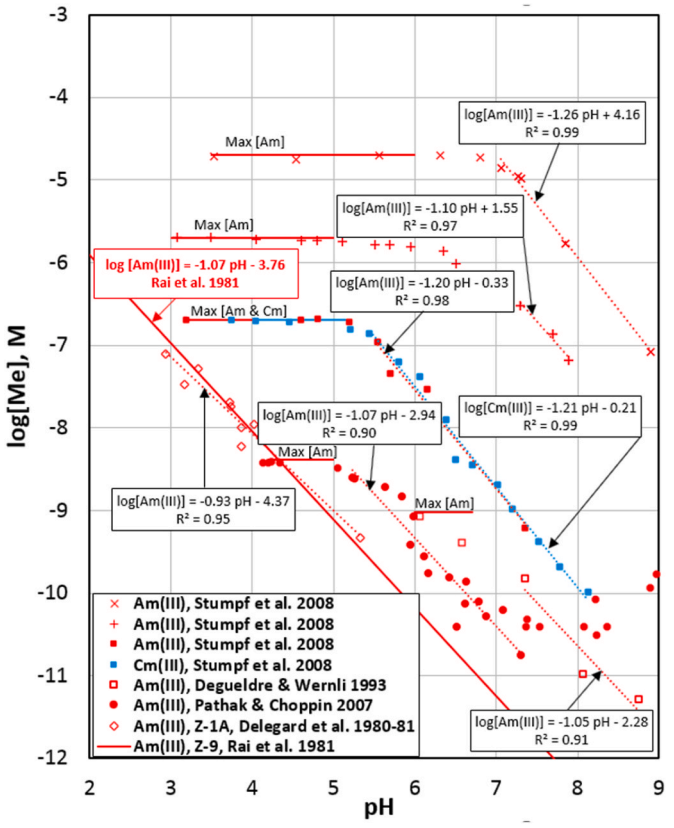


**Fig. 8.** Am(III) (in red) and Cm(III) (in blue) Concentrations in Uptake Equilibria with Finely Crushed Quartz (Stumpf et al., 2008) and Silica Gel (all others) as Functions of pH Compared with Am Concentrations in Leaching Equilibria with Z-9 and Z-1A Sediments.

Z-9 and Z-1A sediments Rai et al., (1981) and Delegard et al. (1980-81 unpublished data) had much greater solid/solution ratios, at 100 g/L and 500–1000 g/L, respectively, than used in the trivalent actinide uptake testing onto amorphous silica or finely divided crushed quartz reported in the technical literature (1–50 g/L). However, the Am-bearing Z-9 and Z-1A sediments contain relatively little finely divided or amorphous silica (even though quartz is present at

appreciable levels in Hanford sediment) compared with the published uptake experiments using pure amorphous silica or fine crushed quartz.

In further leach experiments, Delegard et al. (1980-81 unpublished data) investigated the effects on pH and Am concentration of varying, by about a factor of 15, Z-1A sediment/0.01 M $CaCl_2$ solution ratios. Equilibration time was approximately two weeks. Reflecting the contaminated sediment's acidity, the pH decreased and Am concentrations increased as the sediment/solution ratio increased (Fig. 9). It is clear in Fig. 9, however, that the Am concentrations leached in these tests are lower than observed in the kinetics test using the same 0.01 M $CaCl_2$ leachant at a comparable solid/solution ratio and likewise lower than would be expected based on the log [Am] versus pH correlation established by Rai et al. (1981).

Nothing in the ~40-year-old notebook records reveals the reason for this disparity in amount of Am leached from the Z-1A sediments in the two test types. The most likely explanation is that a less-contaminated (lower Am concentration) Z-1A sediment sample was used in the sediment/solution ratio test series. This interpretation is supported not only by the lower Am concentrations but also by the higher pH (4.01) observed for the 608 g sediment/liter ratio test compared with pH 3.86 in the kinetics test at 555 g sediment/liter solution. It is also clear in Fig. 9 that steady state in the Am concentration and pH are established quickly, within about 8 min (the samplings occurred at 2, 8, 35, 69, 1429, and 10640 min in the kinetics series). Therefore, the disparity is not due to the longer, two-week, equilibration times in the ratio tests compared with the 2-min to ~1 week equilibration times sampled in the kinetics test.

Because the pH was not constant for the sediment/solution ratio experiments, the observed Am concentrations were adjusted to values they would have at pH 4.00 based on the dependence of log [Am] decreasing with increasing pH at a slope of − 1. At the adjusted pH 4.00, the Am concentrations increase in direct proportion to the sediment/solution ratio up to 2.1 g/mL (Fig. 10) with about $1.65 \times 10^{-12}$ mol of Am entering solution per gram of sediment. The single kinetics experiment with 0.01 M $CaCl_2$ (described in Fig. 2 and illustrated again in Fig. 9) showed about five-times more Am going into solution, $7.87 \times 10^{-12}$ mol of Am/gram sediment (Fig. 10), than what was observed in the sediment/solution ratio test series. Based on $1.21 \times 10^{-10}$ mol of total Am/gram sediment loading, ~6.5% of the sediment's Am leached in this single kinetics test.

The linear dependence of Am concentration up to at least 2.1 g/mL solid/solution ratio is noteworthy. First, it showss that the Am solution concentration is not subject to a solubility-controlling solid phase. Second, this linear dependence should hold for any of the contaminated Z-1A sediments and likely those of the chemically and mineralogically similar Z-9 sediments. This means that a small portion of the $Am^{3+}$ on the contaminated sediment, a portion that decreases with increasing pH, enters solution like a freely soluble salt and that the Am solution concentration increases with increase in the sediment/solution ratio. However, even at low pH, most of the Am remains associated with the sediment solids.

The dependence of $Am^{3+}$ concentration on the Z-1A sediment/solution ratio (Fig. 10) plausibly explains the enhanced Am concentrations observed early in the column leach tests (Fig. 3). Delegard et al. (1982) postulated that the high initial Am leach concentration may have been caused by a dissolved complexing agent at the solution front. But the leachate first exiting the column had (180 g)/(0.0342 L = ) 5260 g/L sediment/solution ratio, about 5–10 times greater than the ~500–1000 g/L ratios used in the batch experiments. As shown in Fig. 3, the Am concentration at one pore volume; i.e., the first solution exiting the column; was about 11-times higher than that predicted by batch experiments for 0.01 M $CaCl_2$ (tests done at 555 g sediment/liter) and about 10-times the batch experiment prediction for the simulated groundwater. These findings thus agree in direction and magnitude with the sediment/solution ratio trend shown in Fig. 10.

The metal ion uptake literature data suggest that $Am^{3+}$ interacts with

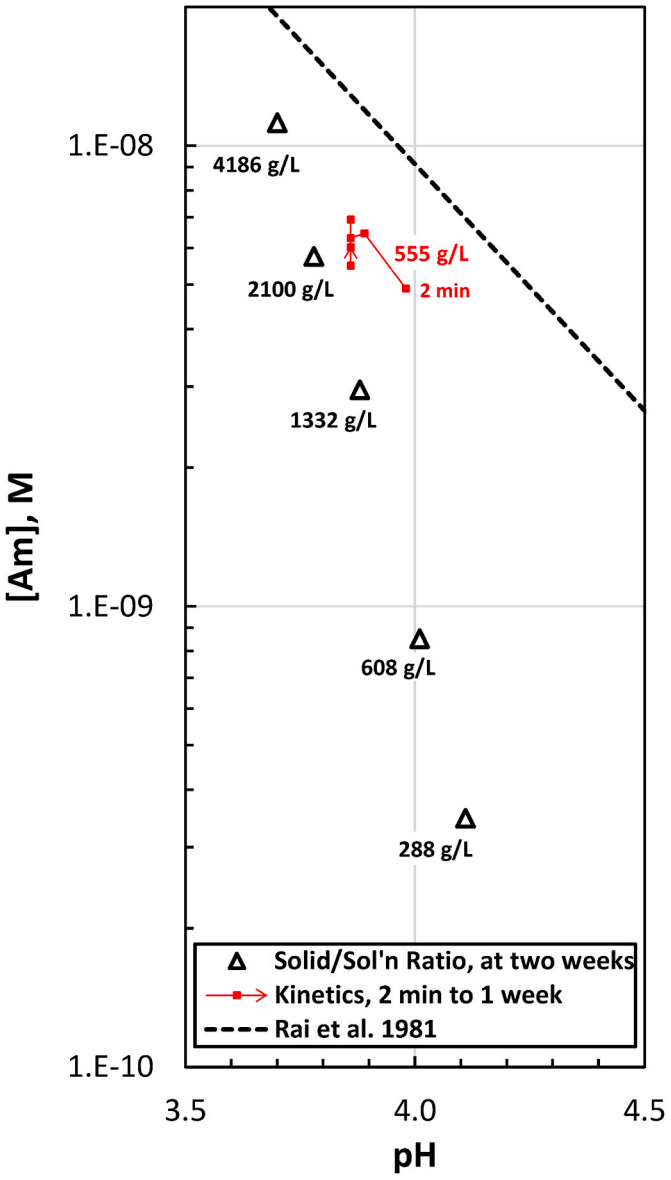


**Fig. 9.** Americium concentrations as functions of sediment/solution ratio and equilibration time for Z-1A sediment contacts in 0.01 M $CaCl_2$ for ratio (black) and kinetics (red).

amorphous silica by ion exchange with the hydrogen ion, $H^+$, from the silanol group, ≡Si–O–H. This surface complexation reaction (Chapter 2 of Stumm 1992) is shown in Equation (6):

$$\equiv Si\text{–}O\text{-}Am^{2+}_{solid} + H^+ \rightleftharpoons \equiv Si\text{–}O\text{-}H_{solid} + Am^{3+} \quad (6)$$

The $Am^{3+}$ ion is electrostatically attracted to silanol's weakly acidic conjugate base (≡Si–$O^-$) in the uptake tests, with $H^+$ increasingly displacing $Am^{3+}$ from the silica gel solid phase as $H^+$ concentration increases. It is noted that the pH of the point of zero charge for Aerosil 200 is < 2.5 to 1 (Kosmulski 2009), thus making cation exchange with silica gel possible in the ≥ pH 3 leach experiments with Z-9 and Z-1A sediments.

Figs. 6, 7, 8, S.1, and S.2 show that other metallic cations sorb similarly and follow equilibria analogous to Equation (6), though to varying degrees. The present interpretation of metal ion sorption on silica gel is not novel, having been made previously by Ahrland et al. (1960) and Schindler et al. (1976; SI). Metal ions' affinities for the weakly acidic silica gel increase with their increasing tendencies to

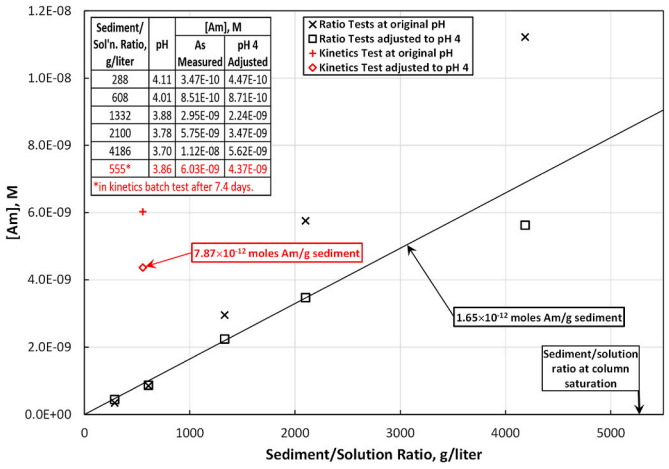


**Fig. 10.** Observed and pH 4 Adjusted Americium Concentrations as Functions of Sediment/Solution Ratio for Z-1A Sediments in 0.01 M $CaCl_2$ after Two Weeks (black) and 7.4 Days (red).

hydrolyze, in the order $Na^{+}<Ca^{2+}<Gd^{3+}<UO_2^{2+}<U^{4+}\sim Pu^{4+}<Zr^{4+}$ (Ahrland et al., 1960). Schindler et al. (Fig. 4; 1976; see also SI) observed affinities for silica uptake increasing in the order $Cd^{2+}<Cu^{2+}<Pb^{2+}<Fe^{3+}$ and noted the linear relationship of the logarithm of the surface complexation reaction constant with the logarithm of the corresponding hydrolysis constant. Such "Linear Free Energy Relationships" (LFER) have since been used as a first step in assessing surface complexation sorption phenomena (e.g., Wang et al., 2001; Romanchuk and Kalmykov 2014).

Thus, the pH of first hydrolysis for these ions (Fig. 11) corresponds in order and approximate magnitude to their observed tendencies to sorb onto silica gel. Although the data for Takahashi et al. (1999; see SI) are less distinct, the trends for the trivalent ions (except for $Ce^{3+}$, which may have been $Ce^{4+}$) also are generally in keeping with first hydrolysis constants. The behaviors of $Am^{3+}$ and $Cm^{3+}$ are analogous to the trivalent rare earth ions $Gd^{3+}$, $Eu^{3+}$, and $Lu^{3+}$.

Leaching of exchangeable Am from contaminated sediments in experiments by Rai et al. (1981) and Delegard et al. (1980–81) has the same −1 slope for plots of log $[Am^{3+}]$ versus pH as observed in the literature for uptake of $Am^{3+}$ and other metal ions onto silica. However, as shown in Fig. 10, relatively low $Am^{3+}$ leachate concentrations arise compared with the total Am present in the contaminated sediments. For this exchangeable Am, the amount dissolved depends only on the contaminated sediment quantity and the $H^{+}$ activity, and thus Am initially dissolves like a freely soluble salt from the contaminated sediment in a way analogous to dissolving sodium chloride from dry sea sand.

The close correspondence of the log [Am]-versus-pH data of Rai et al. (1981) and Delegard et al. (1982) shown in Fig. 2 led both research teams to suppose solubility controls explained the entrancingly coincident data. Though both data sets show the linear log [Am] versus pH relationship with a slope of −1 later observed by others for Am uptake onto silica (Degueldre and Wernli 1993; Pathak and Choppin 2007; Stumpf et al., 2008), the overlying log [Am]-versus-pH data of the Rai et al. (1981) and Delegard et al. (1982) studies now appears to be merely coincidental, not due to solubility control but made comparable by offsetting experimental and material conditions under Am sorption displacement conditions. First, the tests of Rai et al. (1981) and Delegard et al. (1980–82) used arbitrarily different sediment/solution ratios (Table 2). Furthermore, water-washing the tested Z9-4-5A and Z9-4-11A sediment samples, not done in the Z-1A tests, undoubtedly removed appreciable quantities of Am, thus altering the amounts of Am available in the subsequent leach tests by Rai et al. (1981). Despite the washing, the Am concentrations in the two tested Z-9 sediments still were greater

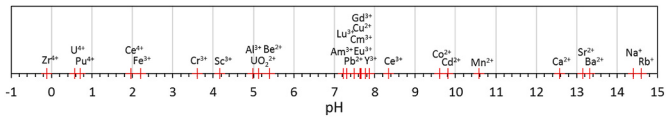


**Fig. 11.** pH of First Hydrolysis Constants for Various Metal Ions at 25 °C and Zero Ionic Strength
(data from Brown and Ekberg 2016).

than that in the Z-1A sediment by factors of about 80 and 150 (Table 2). The five-fold lower Am batch leach concentrations at pH 4 for the sediment/solution ratio tests compared with the kinetics tests for two apparently different Z-1A sediment samples also argue against a solubility control (Figs. 9 and 10). As described in the Stumpf et al. (2008) findings, Fig. 8, at otherwise identical conditions, 10-fold higher available Am concentrations displace the descending log [Am]-versus-pH plots upwards 100-fold.

## 5. Americium retention in the solid phase

Although displacement of a portion of the $Am^{3+}$ from the Z-1A sediment during column leaching experiments can be explained by ion exchange from mineral surfaces, 70% of the Am as well as 99% of the Pu remained with the solids in the column tests, even after passage of 210 column pore volumes of 0.01 M $CaCl_2$ or simulated groundwater leachant (Delegard et al., 1982). Therefore, both Am and Pu must have been present in a form or forms not readily dissolved from the solid phase.

Three alternative arguments can be offered to explain the leach-resistance of the residual Am. One alternative is that the residual $^{241}Am$ was retained in host $PuO_2$ or another low-solubility Pu solid phase (Emerson et al., 2021). The second alternative is that the $H^{+}$ necessary to fully displace the $Am^{3+}$ from the solid according to the reaction in Equation (6) was chemically insufficient in the leachant for the sediments to be leached. The third alternative is that Am was incorporated into a host mineral solid phase, possibly within amorphous silica.

With 70% of the Am and 99% of the Pu remaining in the solid after column leaching, the Pu/Am mass ratio is 86, compared with 64 for the original Z-1A sediment sample. The observed Pu/Am mass ratio of 86 is near the mass ratio of 100 calculated for 9% $^{240}Pu$ (50/50 mix of weapon-grade and fuel-grade Pu) after one $^{241}Pu$ half-life.[6] Based on the observed Pu/Am mass ratio, retention of $^{241}Am$ within a poorly leached Pu solid phase therefore is plausible. However, for an Am-bearing Pu solid phase to be the host, these solids would have had to migrate through a 9-m-thick bed filter of fine sand and silt. Though possible, migration of Am-bearing Pu solids through 9 m of sediment but not through the 22-cm long experimental column is implausible. Therefore,

[6] Operations at PRF were optimized for Pu recovery and purification, including purification from in-grown Am. In addition, Am and trace residual Pu were recovered from PRF raffinates by solvent extraction in the Americium Recovery Building (242-Z; Delegard et al., 2019). Therefore, the relative Am and Pu quantities in wastes disposed to Z-1A do not necessarily represent their quantities in the feed materials. Nevertheless, it is useful to know that recovery of both weapons- and reactor-grade Pu occurred at the PRF from May 1964 until April 1969, with wastes disposed to the Z-1A tile field (Sections 12 and 15 of Gerber, 1997). Hanford N Reactor product Pu in a 50:50 mixed weapons- and fuels-grade Pu (i.e., 9% $^{240}Pu$) would be ~2% $^{241}Pu$ at reactor discharge, and thus ~1% $^{241}Am$ (a Pu/Am mass ratio of ~100) after one 14-year $^{241}Pu$ half-life, the approximate interval between 1964 and 1969 process waste receipt in Z-1A and the ~1979 characterization work. If the waste were solely from weapons-grade (6% $^{240}Pu$) processing and the fractions of Pu and Am lost to waste identical, the Pu/Am mass ratio after one $^{241}Pu$ half-life would be ~230 and ~59 if from fuels-grade 12% $^{240}Pu$ (pages H15, G15, and I15 of Hedengren and Goldberg 1987).

the incorporation of a significant portion of the Am within leach-resistant host $PuO_2$ or another low-solubility Pu phase is unlikely.

The amount of $H^+$ in the Z-1A sediment samples in the column leaching tests may have been chemically insufficient to displace $Am^{3+}$ from the silica solids according to Equation (6). However, as shown in Fig. 3, although the pH of the leachates from the 0.01 M $CaCl_2$ column increased with throughput up to about four column volumes, in the final 195 pore column volumes, or ($195 \times 0.0342$ L = ) ~6.7 L, the pH leveled at about 4.2–4.3, to provide, in this interval, $\sim 1.5 \times 10^{-10}$ M Am. Overall, $\sim 1 \times 10^{-9}$ mol of Am dissolved, about 5% of the ($180\ g \times 1.21 \times 10^{-10}$ mol Am/g = ) $2.18 \times 10^{-8}$ mol of Am initially in the column. In contrast, pH 4.2–4.3 leachant during the initial leaching in this column test (1–2 column pore volumes of throughput) released $\sim 3 \times 10^{-8}$ M Am, 200-times greater Am concentration than observed in the final 195 pore volumes of leachant at the same pH. Together, these findings show that the high retention of Am, even after 210 pore volumes of leachant, is not because of inadequate $H^+$ to satisfy Equation (6), nor because of inadequate solution-sediment equilibration/contact time (about 6.7 h), but instead is because the remaining Am is more difficult to dissolve.

The third alternative is that $Am^{3+}$ becomes incorporated within silica in the Z-9 and Z-1A sediments. Incorporation of $Eu^{3+}$, $Cm^{3+}$, and other metal ions within silica has been observed as described in the technical literature. Incorporation of $Eu^{3+}$ within silica was found to increase with time, as confirmed by laser-induced fluorescence spectroscopy, which demonstrated differences in the $Eu^{3+}$ hydration sphere according to its disposition as dissolved, surface-adsorbed, and silica-incorporated species (Takahashi et al., 2006). This $Eu^{3+}$ was incorporated as individual non-adjacent ions rather than Eu clusters or discrete precipitates, though higher aqueous concentrations may lead to surface precipitation, as observed previously for Eu, which may incorporate into silica over time (Mason et al., 2016).

Similar changes in the $Cm^{3+}$ hydration sphere by its incorporation within silica deposited onto finely crushed quartz were observed by time resolved laser fluorescence spectroscopy (Stumpf et al., 2008). They found that the $Cm^{3+}$, once incorporated, could not be made mobile. Although the spectroscopic findings were consistent with full incorporation by precipitated silica, $Cm^{3+}$ sorbed onto the crushed quartz surface to be blanketed by silicic acid also was offered to explain their data.

Similar findings for the incorporation of metal ions within silica gels has been described for hydrous silica deposited on a natural granite surface in a mine tailings pond (Schindler et al., 2009). The deposit arose by attack of the underlying rock by mine tailings water made acidic (pH 2.6) with sulfuric acid generated by oxidation of sulfide minerals in the tailings. Given the known affinity of trace metal ions to ferric (hydr) oxide scavengers, it is noteworthy that the silica deposits contained Cr, Co, Mn, Ni, Cu, Zn, and Pb at concentrations greater than found on schwertmannite [an Fe(III) (hydr)oxide sulfate mineral] deposits at the same site. Analytical techniques could not distinguish as to whether the trace metals were finely distributed within the silica or present as discrete nucleated (hydr)oxide phases (Schindler et al., 2009). Pan et al. (2021) characterized minerals from natural uranium deposits and suggested that uranyl ion co-precipitation with silica may lead to uranium mineralization and silicification over time.

Overall, the findings of Takahashi et al. (2006) and Mason et al. (2016) for $Eu^{3+}$, Stumpf et al. (2008) for $Cm^{3+}$, Pan et al. (2021) for $UO_2^{2+}$, and Schindler et al. (2009) for Pb and various polyvalent transition metal ions all indicate that metal ions, with time, can incorporate within amorphous silica. Based on these findings, similar incorporation of $Am^{3+}$ into silica might be expected in Hanford sediments such as those in the Z-1A and Z-9 disposal sites.

Finally, as noted, silica-rich chemical alteration zones correlate with areas of high alpha activity, as shown by autoradiolysis images of Z-1A tile field sediment particles retrieved 1.8 m below the waste discharge horizon (Fig. 4). The acid-corroded basalt particle surface is depleted in Ca ~ K ~ Al > Mg > Fe leaving relatively unaltered Si and Ti levels of high alpha activity. Corresponding to high Pu (and perhaps Am) deposition. Of the three alternative explanations provided in this paper for the high retention of Am and Pu in the Z-1A sediment column leaching studies, incorporation of Am and Pu within silica gels is the most plausible.

## 6. Conclusions

Rai et al. (1981) leached waste-contaminated sediments obtained from Hanford's 216-Z-9 covered trench and found that log [Am] versus pH decreased linearly at a slope near −1. They noted similar log [Am] versus pH behavior in early results of Delegard et al. (1980–1981; 1982) leaching of Hanford 216-Z-1A contaminated sediments and others' observations of Am uptake onto a variety of silicate minerals. The Am concentration is established quickly, within one day in the tests by Rai et al. (1981) and, as shown by previously unpublished work by Delegard et al., within a few hours. Based on these findings, Rai et al. (1981) proposed the existence of an undefined but distinct solid phase to control Am concentrations in equilibrium with Hanford PFP waste-contaminated sediments and with minerals in general. They also suggested $Am(OH)_2^+$ as the solution species present in contact with the contaminated sediments. As shown here, reviewed thermodynamic data indicate that $Am^{3+}$, not $Am(OH)_2^+$, is the major solution species present in these leach and uptake tests conducted at pH 3 to 8, except if $PO_4^{-3}$ is present. Reviewed published data, as compared with observations from the Rai et al. (1981) and Delegard et al. (1980–1981; 1982) tests also indicate that the hypothetical Am concentration-controlling solid phase cannot be $Am(OH)_3$ or $AmPO_4 \bullet xH_2O$ and is highly unlikely to be a mixed $(Pu/Am)O_2$ hydrated oxide.

The present study hypothesizes that amorphous silica, a solid phase present naturally in weathered silicate minerals, produced by acid attack in the Z-9 and Z-1A sediments, and part of the disposed Hanford PFP wastes, may plausibly control Am and Pu solution concentration with the log [Am]-versus-pH dependence discovered by Rai et al. (1981). To investigate this hypothesis, literature data on the sorption of $Am^{3+}$, $Cm^{3+}$, chemically analogous trivalent lanthanide ions, and other metal ions onto silica gel, amorphous silica, and finely divided quartz have been examined. The uptake data are presented in plots of log $[Me]_{solution}$ versus pH. These plots, irrespective of metal ion and charge, showed the same −1 slope that Rai et al. (1981) and Delegard et al. (1982) observed for $Am^{3+}$. Stumpf et al. (2008) showed that under otherwise identical experimental conditions the uptake behaviors of $Am^{3+}$ and $Cm^{3+}$ were identical, as would be expected for these neighboring trivalent actinide ions.

The $Am^{3+}$ solution concentration in batch leaching of contaminated Z-1A sediment was found to be directly proportional to the sediment/solution ratio up to at least ~2 kg sediment/liter of leachant and further increasing up to ~4.2 kg/L, with the displaced Am behaving like a freely soluble salt. Significantly, these findings of increasing Am concentration with sediment solution ratio show that Am concentration is not controlled by the solubility of an Am-bearing compound and thus must be controlled by sorption. The $Am^{3+}$ concentration proportionality with sediment/solution ratio also plausibly explains published column leach experiments with Z-1A sediment (Delegard et al., 1982) that gave higher $Am^{3+}$ concentrations in the initial solution throughput at ~5 kg/L sediment/solution ratio, for the observed pH, than shown in batch leaching tests of the same sediment at ~0.5–1 kg/L ratios.

These findings suggest that the dissoluble portion of the $Am^{3+}$ from the contaminated Z-9 and Z-1A sediments interacts by surface complexation and $H^+$ ion exchange with amorphous silica surfaces. The $Am^{3+}$ exchange reaction on the active silanol group is:

$$\equiv Si\text{–}O\text{-}Am^{2+}_{solid} + H^+ \rightleftharpoons \equiv Si\text{–}O\text{-}H_{solid} + Am^{3+}$$

Numerous published uptake studies show that the $Am^{3+}$ ion, like other metal ions, is electrostatically attracted to silica gel's weakly acidic conjugate base but is displaced from the solid phase by increasing

$H^+$ concentration. The present interpretation for $Am^{3+}$ ion exchange uptake onto silica gel has been proposed previously by Ahrland et al. (1960) for other metal ions' uptakes onto silica gel. For Ahrland et al. (1960), the ions' affinities to silica increase with tendency to hydrolysis in the order $Na^+ < Ca^{2+} < Gd^{3+} < UO_2^{2+} < U^{4+} \sim Pu^{4+} < Zr^{4+}$. For the Schindler et al. (1976; see SI) study of amorphous silica, the order is $Cd^{2+} < Cu^{2+} < Pb^{2+} < Fe^{3+}$ and the logarithms of the surface complexation constants correlate highly with the respective metal ion hydrolysis constants in Linear Free Energy Relationship.

Although the − 1 slope of the log [Am]-versus-pH data is observed in experiments by Rai et al. (1981) and Delegard et al. (1980–1981; 1982), the overlap of these log [Am]-versus-pH data very likely is coincidental. Differences in experimental practice, especially water-washing the leached sediment samples by Rai et al. (1981), altered initial Am loading on the Z-9 contaminated sediment and thus altered the log [Am]-versus-pH plot location. Without this preliminary washing, the Rai et al. (1981) log [Am] - pH data likely would have appeared at greater values and not overlapped the Delegard et al. (1982) values. The Z-1A tests with varied sediment/solution ratios also deviate from the log [Am]-pH relation of previous work (Rai et al., 1981).

The incomplete removal of $Am^{3+}$ from the contaminated Z-1A sediment, even with extensive column leaching, suggests that $Am^{3+}$ is not merely present in the solid phase(s) by surface complexation but also is incorporated within refractory Pu solid phases (e.g., $PuO_2$) or, for both Am and Pu, by occlusion within amorphous silica via its continuing dynamic dissolution and reprecipitation. This latter mechanism is more plausible and would be particularly active for moderately soluble (2 mM) amorphous silica. Published studies show $Eu^{3+}$, $Cm^{3+}$, and $UO_2^{2+}$ incorporation into amorphous silica increasing with time, as confirmed by parallel decreased ion hydration based on spectral analysis (Takahashi et al., 2006, Stumpf et al., 2008; and Pan et al., 2021, respectively). Incorporation of various transition metal and lead ions from acidic mine tailings ponds into amorphous silica also has been observed (Schindler et al., 2009). Based on these findings, and autoradiography images showing the apparent incorporation of Pu and probably Am within silica-rich mineral residues in waste-affected Z-1A basalt grains (Price and Ames 1976). Appreciable $Am^{3+}$ and Pu incorporation within amorphous silica might be expected in Hanford sediments, such as those in Z-1A and Z-9, to prevent or significantly retard their susceptibility to leaching and thus to migration. Similar incorporations of Am, Pu, and other trace cationic radioactive contaminants within ubiquitous silica in other mineralogical settings to resist leaching and retard migration thus are likely and worthy of investigation.

Future research should focus on identifying the elements and phases with which Am (and Pu) are associated in the Z-9 and Z-1A sediments, i.e., whether it is amorphous silica as posited here or another solid phase such as some form of ferric (hydr)oxide. The concentrations of amorphous silica in these contaminated sediments also should be estimated, such as by dilute sodium hydroxide leaching (Georgiadis et al., 2015). It should be noted that working with these samples is challenging due to their radioactivity, relatively low concentrations of Am and Pu present, and the difficulties in retrieving and characterizing sediments from the waste disposal sites. Therefore, tests of $Am^{3+}$ or analogous $Eu^{3+}$ uptake from simulated PFP wastes onto non-contaminated native Hanford Formation sediments can be performed to assess, using micro-characterization techniques, distributions of these metal ions onto discrete sediment minerals (e.g., silica, plagioclase), waste-origin precipitates, and native mineral alteration products. Potential techniques include atom probe tomography to detect Am, Eu, and, for waste site samples, Pu and Am associations with depth across sediment particles coupled with micro X-ray techniques (including X-ray absorption spectroscopy, X-ray diffraction, and X-ray fluorescence) to identify associated mineral phases. Additional experiments could also be conducted with analogs sensitive to other fluorescence techniques (e.g., Eu) to better understand speciation. These techniques would help to confirm (or reject) our hypothesis for amorphous silica involvement in the leach-resistant fraction of Am (and Pu). For regulatory purposes, tests of waste-contaminated sediments following defined Environmental Protection Agency protocols for contaminant liquid/solid partitioning as a function of pH in batch testing (Method 1313) and partitioning in column leaching (Method 1314) also may be performed (EPA 2012, 2013).

## Declaration of competing interest

The authors declare that they have no known competing financial interests or personal relationships that could have appeared to influence the work reported in this paper.

## Data availability

Data will be made available on request.

## Acknowledgements

C.H.D. gratefully acknowledges the impetus and guidance of R.B. (Bob) Kasper in leading the 1980s work and the support of J.P. (Jim) Sloughter in pursuing continued support in the 1980s. The 1980s work was performed at Rockwell Hanford Operations, Richland, WA, for the US Department of Energy under contract DE-AC06-77RL01030. This document was prepared under the Deep Vadose Zone – Applied Field Research Initiative at Pacific Northwest National Laboratory. The Pacific Northwest National Laboratory is operated by Battelle Memorial Institute for the DOE under Contract DE-AC05-76RL01830.

## Appendix. Supplementary data

Supplementary data to this article can be found online at https://doi.org/10.1016/j.apgeochem.2023.105690.

## References

Ahrland, S., Grenthe, I., Norén, B., 1960. The ion exchange properties of silica gel. I. The sorption of $Na^+$, $Ca^{2+}$, $Ba^{2+}$, $UO_2^{2+}$, $Gd^{3+}$, Zr(IV) + Nb, U(IV) and Pu(IV). Acta Chem. Scand. 14, 1059–1076. https://doi.org/10.3891/acta.chem.scand.14-1059.

Alexander, G.B., Heston, W.M., Iler, R.K., 1954. The solubility of amorphous silica in water. J. Phys. Chem. 58 (6), 453–455. https://doi.org/10.1021/j150516a002.

Alfredsson, H., Clymans, W., Hugelius, G., Kuhry, P., Conley, D.J., 2016. Estimated storage of amorphous silica in soils of the circum-arctic tundra region. Global Biogeochem. Cycles 479–500. https://doi.org/10.1002/2015GB005344.

Allard, D.B., Beall, G.W., Krajewski, T., 1980. Sorption of actinides in igneous rocks. Nucl. Technol. 49, 474–480. https://doi.org/10.13182/NT80-A17695.

Ames, L.L., 1974. *Characterization of Actinide Bearing Soils: Top Sixty Centimeters of 216-Z-9 Enclosed Trench.* BNWL-1812, Battelle Pacific Northwest Laboratories. Richland, WA. https://www.osti.gov/biblio/4313915-characterization-actinide-bearing-soils-top-sixty-centimeters-enclosed-trench.

Brown, P.L., Ekberg, C., 2016. Hydrolysis of Metal Ions. Wiley-VCH Verlag GmbH & Company, Weinheim, Germany.

Degueldre, C., Wernli, B., 1993. Association behaviour of $^{241}Am(III)$ on $SiO_{2\ (amorphous)}$ and $SiO_{2\ (quartz)}$ colloids. J. Environ. Radioact. 20, 151–167. https://doi.org/10.1016/0265-931X(93)90007-T.

Delegard, C.H., Gallagher, S.A., Kasper, R.B., 1982. Saturated column leach studies: Hanford 216-Z-1A sediment. In: Presented at *International Symposium on the Migration in the Terrestrial Environment of Long-Lived Radionuclides*, 27-31 July 1981, and in the Proceedings of that Meeting, Environmental Migration of Long-Lived Radionuclides, International Atomic Energy Agency, Proceedings Series STI/PUB/597. Also as RHO-SA-210, 1981. Rockwell Hanford Operations, Richland, WA. https://www.iaea.org/publications/3431/environmental-migration-of-long-lived-radionuclides-knoxville-27-31-july-1981. osti.gov/biblio/6279493, respectively. Previously unpublished data from laboratory notebooks RHO-N-149, assigned to SA Gallagher, 20 July 1978, and RHO-RDN-112, assigned to CH Delegard 7 October 1980, also used.

Delegard, C.H., Emerson, H.P., Cantrell, K.J., Pearce, C.I., 2019. *Generation and Characteristics of Plutonium and Americium Contaminated Soils and Underlying Waste Sites at Hanford.* PNNL-29203, DVZ-RPT-0024 Rev 0.0, Pacific Northwest National Laboratory. Richland, WA. https://www.pnnl.gov/main/publications/external/technical_reports/PNNL-29203.pdf.

Emerson, H.P., Pearce, C.I., Delegard, C.H., Cantrell, K.J., Snyder, M.M.V., Thomas, M.-L., Gartman, B.N., Miller, M.D., Resch, C.T., Heald, S.M., Plymale, A.E., Reilly, D.D., Saslow, S.A., Nelson, W., Murphy, S., Zavarin, M., Kersting, A.B., Freedman, V.L., 2021. Influences on subsurface plutonium and americium migration. ACS Earth and Space Chem. 5 (2), 279–294. https://doi.org/10.1021/acsearthspacechem.0c00277.

Emerson, H.P., Sinkov, S.I., Pearce, C.I., Cantrell, K.J., Delegard, C.H., Snyder, M.M.V., Thomas, M.-L., Reilly, D.D., Buck, E.C., Sweet, L., Casella, A.J., Carter, J.C., Corbey, J.F., Schwerdt, I.J., Clark, R., Heller, F.D., Meier, D., Zavarin, M., Kersting, A.B., Freedman, V.L., 2022. Solubility controls on plutonium and americium release in subsurface environments exposed to acidic processing wastes. Appl. Geochem. 105241 https://doi.org/10.1016/j.apgeochem.2022.105241 (in press).

EPA, 2012. Liquid-Solid Partitioning as a Function of Extract pH Using a Parallel Batch Extraction Procedure". Environmental Protection Agency, Washington DC. Method 1313. https://www.epa.gov/sites/default/files/2015-12/documents/1313.pdf.

EPA, 2013. Liquid-Solid Partitioning as a Function of Liquid-Solid Ratio for Constituents in Solid Materials Using an Up-Flow Percolation Column Procedure". Environmental Protection Agency, Washington DC. Method 1314. https://www.epa.gov/sites/default/files/2015-12/documents/method_1314_final_03-22-13.pdf.

Felmy, A.R., Schroeder, C.C., Mason, M.J., 1994. A solubility model for amorphous silica in concentrated electrolytes. In: Presented at *Symposium of Scientific Issues Related to Safety and Treatment of Hanford Tank Wastes*, Washington, DC, August, 1994. Pacific Northwest Laboratory, Richland, WA. http://www.osti.gov/scitech/servlets/purl/10110157-3hjADX/webviewable/.

Georgiadis, A., Sauer, D., Breuer, J., Herrmann, L., Rennert, T., Stahr, K., 2015. Optimising the extraction of amorphous silica by NaOH from soils of temperate-humid climate. Soil Res. 53, 392–400. https://doi.org/10.1071/SR14171.

Gerber, M.S., 1997. *History and Stabilization of the Plutonium Finishing Plant (PFP) Complex, Hanford Site*. HNF-EP-0924, Fluor Daniel Hanford. Incorporated, Richland, WA. http://www.osti.gov/scitech/biblio/325360.

Grenthe, I., Gaona, X., Plyasunov, A.V., Runde, W.H., Konings, R.J.M., Moore, E.E., Rao, L., Grambow, B., Smith, A.L., 2020. Second Update on the Chemical Thermodynamics of Uranium, Neptunium, Plutonium, Americium, and Technetium. OECD Nuclear Energy Agency, Paris, France. https://www.oecd-nea.org/jcms/pl_46643/second-update-on-the-chemical-thermodynamics-of-u-np-pu-am-and-tc.

Guillaumont, R., Fanghänel, T., Fuger, J., Grenthe, I., Palmer, D.A., Rand, M.H., 2003. Update on the Chemical Thermodynamics of Uranium, Neptunium, Plutonium, Americium and Technetium.

Hedengren, D.C., Goldberg, H.J., 1987. *ORIGEN2 Predictions of N Reactor Fuel Actinide Composition*. RHO-SD-CP-TI-105. Rockwell Hanford Operations, Richland, WA.

Kar, A.S., Tomar, B.S., Godbole, S.V., Manchanda, V.K., 2011. Time resolved fluorescence spectroscopy and modeling of Eu(III) sorption by silica in presence and absence of alpha hydroxy isobutyric acid. Colloids Surf. A Physicochem. Eng. Asp. 378, 44–49. https://doi.org/10.1016/j.colsurfa.2011.01.039.

Kasting, J.F., 2019. The goldilocks planet? How silicate weathering maintains earth "just right". Elements 15, 235–240. https://doi.org/10.2138/gselements.15.4.235.

Kosmulski, M., 2009. pH-dependent surface charging and points of zero charge. IV. Update and new approach. J. Colloid Interface Sci. 337, 439–448. https://doi.org/10.1016/j.jcis.2009.04.072.

Lindsay, W.L., 1979. Chemical Equilibria in Soils. Wiley Interscience, New York, NY.

Mason, H.E., Begg, J.D., Maxwell, R.S., Kersting, A.G., Zavarin, M., 2016. A novel solid-state NMR method for the investigation of trivalent lanthanide sorption on amorphous silica at low surface loadings. Environ. Sci. J. Integr. Environ. Res.: Process. Impacts 18, 802–809. https://doi.org/10.1039/C6EM00082G.

Moulin, V D Stammose, Ouzounian, G., 1992. Actinide sorption at oxide-water interfaces: application to α-alumina and amorphous silica. Appl. Geochem. 1, 163–166. https://doi.org/10.1016/S0883-2927(09)80072-3.

Neck, V., Altmaier, M., Fanghänel, T., 2007. Solubility of plutonium hydroxides/hydrous oxides under reducing conditions and in the presence of oxygen. Compt. Rendus Chem. 10, 959–977. https://doi:10.1016/j.crci.2007.02.011.

Owens, K.W., 1981. *Existing Data on the 216-Z Liquid Waste Sites*. RHO-LD-114. Rockwell Hanford Operations, Richland, WA. https://www.osti.gov/servlets/purl/570355.

Pan, Y., Li, D., Feng, R., Wiens, E., Chen, N., Cherniov, R., Gotze, J., Lin, J., 2021. Uranyl binding mechanism in microcrystalline silicas: a potential missing link for uranium mineralization by direct uranyl Co-precipitation and environmental implications. Geochem. Cosmochim. Acta 292, 518–531. https://doi.org/10.1016/j.gca.2020.10.017.

Pathak, P.N., Choppin, G.R., 2006. Sorption studies of europium(III) on hydrous silica. J. Radioanal. Nucl. Chem. 270 (2), 277–283. https://doi.org/10.1007/s10967-006-0345-9.

Pathak, P.N., Choppin, G.R., 2007. Sorption of $Am^{3+}$ cations on suspended silicate: effects of pH, ionic strength, complexing anions, humic acid and metal ions. J. Radioanal. Nucl. Chem. 274 (3), 517–523. https://doi.org/10.1007/s10967-006-6942-9.

Price, S.M., Ames, L.L., 1976. Characterization of actinide-bearing sediments underlying liquid waste disposal facilities at Hanford. In: Paper IAEA-SM-199/87, Pages 191-211, Transuranium Nuclides in the Environment, STI/PUB/410. International Atomic Energy Agency, Vienna, Austria. Also published in 1975 as ARH-SA-232. https://www.iaea.org/publications/3182/transuranium-nuclides-in-the-environment-san-francisco-17-21-nov-1975. inis.iaea.org/collection/NCLCollectionStore/_Public/07/238/7238004.pdf?r=1&r=1, respectively.

Price, S.M., Kasper, R.B., Additon, M.K., Smith, R.M., Last, G.V., 1979. Distribution of Plutonium and Americium beneath the 216-Z-1A Crib: A Status Report. RHO-ST-17. Rockwell Hanford Operations, Richland, WA.

Rai, D., Strickert, R.G., Moore, D.A., Serne, R.J., 1981. Influence of an americium solid phase on americium concentrations in solutions. Geochem. Cosmochim. Acta 45, 2257–2265. https://doi.org/10.1016/0016-7037(81)90075-2.

Rai, D., Felmy, A.R., Fulton, R.W., 1992. Solubility and ion activity product of $AmPO_4{\cdot}xH_2O$(am). Radiochim. Acta 56, 7–14. https://doi.org/10.1524/ract.1992.56.1.7.

Relyea, J.F., Ames, L.L., Serne, R.J., Fulton, R.J., Washburn, C.D., 1979. Batch $K_d$ Determinations with.

Romanchuk, A.Y., Kalmykov, S.N., 2014. Actinides sorption onto hematite: experimental data, surface complexation modeling and linear free Energy relationship. Radiochim. Acta 102, 303–310. https://doi.org/10.1515/ract-2014-2108.

Schindler, P.W., Fürst, B., Dick, R., Pu, Wolf, 1976. Ligand properties of surface silanol groups I. Surface complex Formation with $Fe^{3+}$, $Cu^{2+}$, $Cd^{2+}$, and $Pb^{2+}$. J. Colloid Interface Sci. 55, 469–475. https://doi.org/10.1016/0021-9797(76)90057-6.

Schindler, M., Durocher, J.L., Abdu, Y., Hawthorne, F.C., 2009. Hydrous silica coatings: occurrence, speciation of metals, and environmental significance. Environ. Sci. Technol. 43, 8775–8780. https://doi.org/10.1021/es9018817.

Shannon, R.D., 1976. Revised effective ionic radii and systematic studies of interatomic distances in halides and chalcogenides. Acta Crystallogr. 32, 751–767. https://doi.org/10.1107/S0567739476001551.

Stumm, W., 1992. Chemistry of the Solid-Water Interface: Processes at the Mineral-Water and Particle-Water Interface in Natural Systems. John Wiley & Sons, Incorporated, New York, NY.

Stumpf, S., Stumpf, Th, Lützenkirchen, J., Walther, C., Fanghänel, Th, 2008. Immobilization of trivalent actinides by sorption onto quartz and incorporation into siliceous bulk: investigations by TRLFS. J. Colloid Interface Sci. 318, 5–14. https://doi.org/10.1016/j.jcis.2007.09.080.

Takahashi, Y., Minae, Y., Ambe, S., Makide, Y., Ambe, F., 1999. Comparison of adsorption behavior of multiple inorganic ions on kaolinite and silica in the presence of humic acid using the multitracer technique. Geochem. Cosmochim. Acta 63 (6), 815–836. https://doi.org/10.1016/S0016-7037(99)00065-4.

Takahashi, Y., Murata, M., Kimura, T., 2006. Interaction of Eu(III) ion and non-porous silica: irreversible sorption of Eu(III) on silica and hydrolysis of silica promoted by Eu(III). J. Alloys Compd. 408–412, 1246–1251. https://doi.org/10.1016/j.jallcom.2005.04.120.

Wang, P., Anderko, A., Turner, D.M., 2001. Thermodynamic modeling of the adsorption of radionuclides on selected minerals. I: cations. Ind. Eng. Chem. Res. 40, 4428–4443. https://doi.org/10.1021/ie000991p.

Xie, Y., Last, G.V., Murray, C.J., Mackley, R., 2003. Mineralogical and Bulk-Rock Geochemical Signatures of Ringold and Hanford Formation Sediments. PNNL-14202. Pacific Northwest National Laboratory, Richland, WA. https://www.pnnl.gov/main/publications/external/technical_reports/PNNL-14202.pdf.